arXiv:1404.3753v2 [stat.ME] 29 May 2014

Multi-resolution two-sample comparison through the divide-merge Markov tree

Jacopo Soriano and Li Ma

Department of Statistical Science

Duke University, Durham, NC 27708

email: jacopo.soriano@duke.edu, li.ma@duke.edu

May 30, 2014

Abstract

We introduce a probabilistic framework for two-sample comparison based on a nonparametric process taking the form of a Markov model that transitions between a "divide" and a "merge" state on a multi-resolution partition tree of the sample space. Multi-scale two-sample comparison is achieved through inferring the underlying state of the process along the partition tree. The Markov design allows the process to incorporate spatial clustering of differential structures, which is commonly observed in two-sample problems but ignored by existing methods. Inference is carried out under the Bayesian paradigm through recursive propagation algorithms. We demonstrate the work of our method through simulated data and a real flow cytometry data set, and show that it substantially outperforms other state-of-the-art two-sample tests in several settings.

KEYWORDS: Bayesian inference; Pólya tree; Nonparametrics; Multi-resolution inference; Hypothesis testing; Flow cytometry.

1 Introduction

Two-group comparison is of fundamental interest in a variety of applications, and over the last few decades, many nonparametric two-sample tests have been invented. Some notable examples include the Kolmogorov-Smirnov test (Bickel, 1969), the k-nearest neighbors test (Schilling, 1986; Henze, 1988), and the Cramér test (Baringhaus and Franz, 2004), among many others. More recently a number of Bayesian methods have been proposed, and in particular a multi-resolution approach based on the Pólya tree (PT) process (Ferguson, 1973; Lavine, 1992) has gained popularity. The PT process decomposes a probability distribution in a wavelet-like fashion into a collection of local probability assignment coefficients on a multi-scale partition sequence of the sample space. Two-sample comparison is then achieved through comparing these local assignments and combining the statistical evidence across the partition sequence to form a global test statistic. Methods following this strategy include Holmes et al. (2012), Chen and Hanson (2012), and Ma and Wong (2011).

The main motivation for this work stems from an important and almost ubiquitous phenomenon in two-sample problems that has not been taken into account by existing methods—the spatial clustering of differential structures. More specifically, if there is two-sample difference at one location in the sample space, then the neighboring parts of the sample space are more likely to contain differential structures as well. Therefore methods for finding two-sample differences across the sample space should ideally incorporate the dependence among the neighboring locations rather than treating them independently. This relates to the more general problem of multiple testing adjustment for dependent hypotheses.

In this work we introduce a new method for two-sample comparison that incorporates this dependence structure to improve power. The core of our method is a new nonparametric process—called the *Divide-Merge Markov Tree* (DMMT)—taking the form of a tree-structured Markov model (Crouse et al., 1998) that transitions between "divide" and "merge"

states on a multi-resolution partition sequence of the sample space, corresponding respectively to whether the two distributions are locally equal or not. The Markov dependence provides a convenient framework for incorporating spatial dependence of differential structures. Under this framework, testing two-sample differences is achieved through inferring the underlying Markov state of the process on different parts of the space.

Moreover, in multivariate problems the DMMT allows the multi-resolution partition sequence on which the Markov tree grows to be data-adaptive. When the sample space is vast, as is common in multi-dimensional problems, fixed, symmetric partition sequences adopted by standard multi-resolution methods quickly run into a sparsity problem—just a few levels down the partition sequence, most sets contain only very few data points. Consequently, on most location-scale combinations there are too few data to draw reliable inference. This sparsity translates into high posterior uncertainty of the underlying states for most sets in the partition sequence and loss of statistical power. To address this challenge, the DMMT adopts a random partitioning mechanism (Wong and Ma, 2010) that allows the partition sequence to be inferred from the data. Interestingly this additional adaptiveness can be achieved without affecting the Markov nature of the process, which is critical for incorporating spatial clustering and efficient posterior inference.

Furthermore, the DMMT process provides a natural means to summarizing and visualizing the inferred difference. We show that one can effectively represent posterior summary of the differential structure by plotting a representative partition sequence of the sample space and highlighting the regions where the two distributions have high posterior probability of being different.

In addition, we formally investigate the theoretical properties of the DMMT model. We show that it satisfies Ferguson's criteria (Ferguson, 1973) for desirable nonparametric processes—it has large support (and so is a nonparametric process) and is analytically tractable (posterior inference can be carried out very efficiently due to its Markov nature).

Moreover, we show that the multi-resolution two-sample test using the DMMT is consistent. Holmes et al. (2012) showed that the multi-resolution approach using the standard PT process gives consistent two-sample tests. Our results further show that this consistency can be maintained while introducing additional flexibility and adaptivity into the underlying model through the Markov design and the adaptive partitioning feature.

The paper is organized as follows. In Section 2 we present our multi-resolution two-sample comparison framework based on the DMMT process. We introduce the DMMT process, establish its theoretical properties, and provide the inferential recipe for carrying out two-sample comparison. We provide guidelines for prior specification. In Section 3 we illustrate the work of our method and evaluate its performance. We first carry out a simulation study to compare the power of our method as a two-sample test to other nonparametric two-sample tests. We also illustrate how to pin-point and visualize where and what the difference is using the posterior process. Finally, we apply our method to analyzing a seven-dimensional cytometry data set, for which our method successfully identifies an experimentally validated differential hotspot involving just 0.2% of the data points. Section 4 closes with a brief discussion.

2 Method

2.1 Some basic concepts and notation on recursive partitioning

Recursive partitioning of the sample space is a fundamental building block for the multi-resolution approach to two-sample comparison (Holmes et al., 2012; Chen and Hanson, 2012; Ma and Wong, 2011). We start by introducing some basic concepts and notation about recursive partitioning that will be used throughout the paper.

Let Ω denote the sample space, which can either be finite such as a contingency table or an Euclidean rectangle. While our proposed method is applicable to both cases, for

simplicity, our presentation will focus on the Euclidean case. Without loss of generality, let $\Omega = [0,1)^p$. An unbounded rectangle can be transformed into a bounded rectangle by applying, for example, a cdf transformation to each dimension.

A *dimensionwise dyadic partition* of $A = [a_1, b_1) \times [a_2, b_2) \times \cdots \times [a_p, b_p) \subset \Omega$ refers to a division of A into two halves by splitting at the middle of the support of one of the p dimensions. For each A, we use $\{A_l^j, A_r^j\}$ to denote the pair of children nodes—called the *left* and *right* children—of A obtained by cutting A along the jth direction. That is, A_l^j is the half with the jth dimension supported on $[a_j, (a_j + b_j)/2)$, and A_r^j is the half with the jth dimension supported on $[(a_j + b_j)/2, b_j)$.

We consider recursive partition sequences of Ω generated by dimensionwise dyadic partitions. Each such partition sequence can be represented by a bifurcating tree. A node in the tree represents a subset of the sample space Ω, and is obtained from a dyadic partition of its parent node. At the top level of the tree, the root (or level-0) node of the tree is the whole space Ω, while at the first level there are two (level-1) nodes obtained by partitioning Ω along one of the p dimensions. Each level-1 node can be partitioned again, defining the next level of the tree and so on.

Let $\mathcal{A}^k$ denote the collection of all level-k nodes under all possible recursive partition sequences of Ω. In other words, it is the set of all possible subsets obtainable by sequentially partitioning the sample space k times. Also, let $\mathcal{A}^{(k)} = \cup_{i=0}^k \mathcal{A}^i$, the collection of all possible nodes up to level k, and $\mathcal{A}^{(\infty)} = \cup_{i=0}^\infty \mathcal{A}^i$, the collection of all possible nodes.

2.2 The divide-merge Markov tree (DMMT)

Next we introduce a generative model for a pair of distributions (Q_1, Q_2), called the divide-merge Markov tree (DMMT). We first describe the general design principle of the process and then provide the mathematical details.

The DMMT model takes a Pólya tree like multi-resolution approach to generating prob-

ability distributions. It divides the sample space into a sequence of nested partitions, and then at each node in the partition tree, it specifies how probability mass is split between the left and the right children. The process uses this strategy to generate both distributions Q_1 and Q_2 simultaneously, and use a hidden Markov model (Crouse et al., 1998) to determine the relationship between the two distributions on each of the node. Under a "divide" state, probability mass is split differently for the two distributions into the two children nodes, while under a "merge" state, the same probability assignment is applied for both distributions. The Markov tree also has an additional "stop" state, representing the case when the two distributions are conditionally equal to some baseline distribution.

Under this design, inference on two-sample comparison can be achieved through learning the divide-merge states of the process across the partition tree. To further allow the partition sequence of the sample space to be data-adaptive *a posteriori* thereby improving statistical power in multivariate problems, the DMMT incorporates a randomized partition mechanism introduced in Wong and Ma (2010).

Given this general design, next we formally describe the DMMT process as a generative procedure in an inductive manner. Suppose the generative procedure has proceeded onto a subset A of Ω. To initiate the induction, $A = \Omega$, the entire sample space. The procedure carries out three operational steps on A:

1. Divide-merge step—to determine its "divide", "merge", or "stop" state on A;
2. Random partitioning step—to determine how to further partition A into children;
3. Probability assignment step—to determine how Q_1 and Q_2 assign probability to A's children.

Next we describe each of the steps in turn. Figure 1 provides an illustration to help the reader understand the technical description.

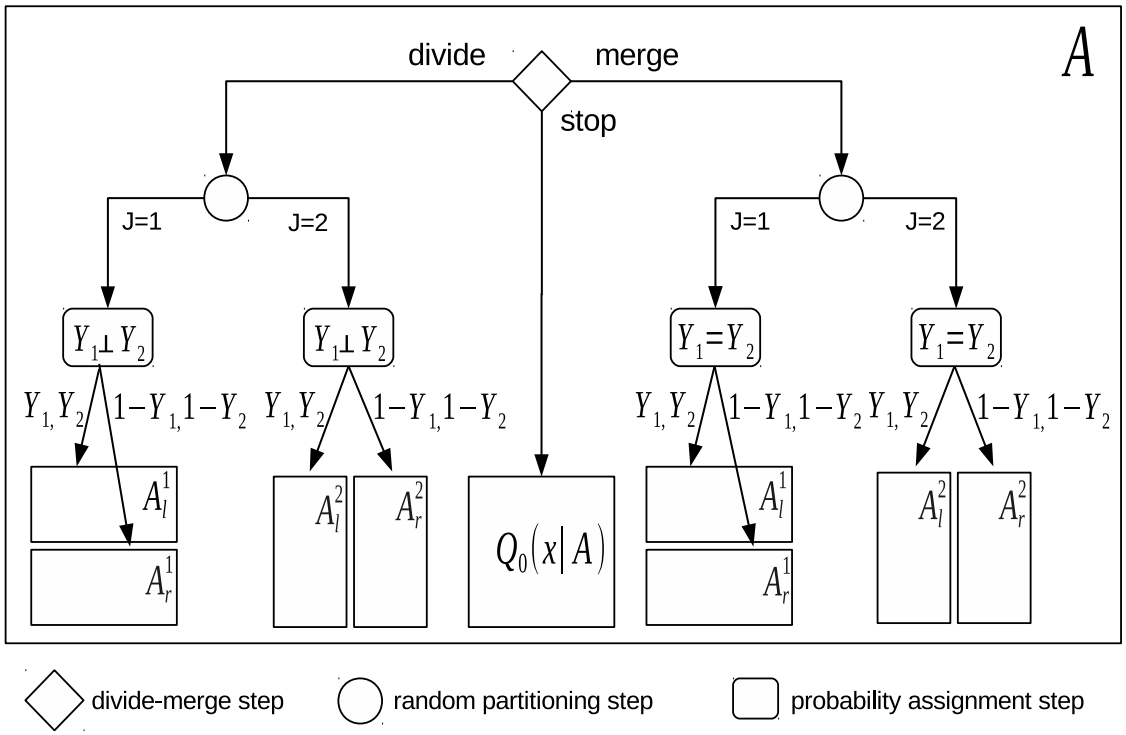

Figure 1: The three steps of the DMMT generative procedure for a set $A \in \mathcal{A}^{(\infty)}$.

Divide-merge step The procedure can take one of three states: "divide", "merge" and "stop" on A. Define the set of the states $\mathcal{G} = \{d, m, s\}$. Consider $h \in \mathcal{G}$ being the state of the parent of A. We draw a random variable to determine the state of the process on A:

$$\Pr\left[S(A) = g | S(\text{parent}(A)) = h\right] = \rho_{h,g}(A),$$

where $\rho_{h,g}(A) \geq 0$ for any $g, h \in \mathcal{G}$, and $\sum_g \rho_{h,g}(A) = 1$ for any $h \in \mathcal{G}$. We call $\rho_{h,g}(A)$ the transition probabilities, and organize them in a transition probability matrix

$$\boldsymbol{\rho}(A) = \begin{bmatrix} \rho_{d,d}(A) & \rho_{d,m}(A) & \rho_{d,s}(A) \\ \rho_{m,d}(A) & \rho_{m,m}(A) & \rho_{m,s}(A) \\ \rho_{s,d}(A) & \rho_{s,m}(A) & \rho_{s,s}(A) \end{bmatrix}.$$

The procedure will terminate once in the "stop" state, and so by construction $\rho_{s,d}(A) = \rho_{s,m}(A) = 0$ and $\rho_{s,s}(A) = 1$. The root of the tree Ω does not have a parent, so we draw its "parent" state from a multinomial Bernoulli corresponding to "initial" state probabilities $(\rho_{0,d}, \rho_{0,m}, \rho_{0,s})$.

Random partitioning step If the process "stops" on A, i.e. $S(A) = s$, then A is not further partitioned. Otherwise, if $S(A) = g$ for $g \in \{d, m\}$, we draw a partition direction $J(A)$ according to

$$\Pr\big(J(A) = j | S(A) = g\big) = \lambda_j(A, g),$$

where $\lambda_j(A, g) \geq 0$ for $j = 1, \ldots, p$ and $\sum_j \lambda_j(A, g) = 1$ for $g \in \{d, m\}$, and we make a dimensionwise dyadic partition in dimension j and obtain two subsets A_l^j and A_r^j. It may look intriguing that the partition probability $\lambda_j(A, g)$ should be allowed to depend on the state g. We will see later that under $g = m$, the partition characterizes the common structure of the two distributions, while under $g = d$, their difference.

Probability assignment step The probability assignment depends on the state of the process. If $S(A) = d$, we generate two independent Beta variables $Y_1(A)$ and $Y_2(A)$ such that

$$Y_t(A) \sim \text{Beta}\big(\boldsymbol{\alpha}_t^j(A, d)\big),$$

where $\boldsymbol{\alpha}_t^j(A, d) = \big(\alpha_{t,l}^j(A, d), \alpha_{t,r}^j(A, d)\big)$ are the pseudo-counts parameters, which can be different for $t = 1$ and 2. Otherwise, if $S(A) = m$, we generate

$$Y_1(A) = Y_2(A) \sim \text{Beta}\big(\boldsymbol{\alpha}^j(A, m)\big),$$

where $\boldsymbol{\alpha}^j(A, m) = \big(\alpha_l^j(A, m), \alpha_r^j(A, m)\big)$ are the pseudo-counts parameters. For $t = 1$ and 2, we assign a proportion equal to $Y_t(A)$ and $1 - Y_t(A)$ of the probability that Q_t assigns to A to the left and right children, respectively:

$$Q_t(A_l^j) = Q_t(A)Y_t(A), \quad Q_t(A_r^j) = Q_t(A)(1 - Y_t(A)).$$

Finally, if $S(A) = s$, then for both Q_1 and Q_2, probability is assigned on A accordingly to a baseline distribution Q_0

$$Q_1(\cdot|A) = Q_2(\cdot|A) = Q_0(\cdot|A).$$

This completes the inductive description of the procedure on A. If the procedure does not stop on A, then it proceeds onto applying the same three-step operation on each of A's children. The generative model is completely specified by the three sets of parameters $\boldsymbol{\rho}(A)$, $\lambda_j(A, g)$ and $\boldsymbol{\alpha}_t^j(A, g)$ for $j = 1, \ldots, p$, $t = 1, 2$, $g \in \{d, m\}$ and $A \in \mathcal{A}^{(\infty)}$. From now on we will write these three sets of parameters as $\boldsymbol{\rho}$, $\boldsymbol{\lambda}$ and $\boldsymbol{\alpha}$ respectively.

If the prior probability of stopping is uniformly bounded away from zero, i.e. there exists $\delta > 0$ such that $\rho_{g,s}(A) > \delta$ for all $A \in \mathcal{A}^{(\infty)}$ and $g \in \mathcal{G}$, then with probability 1 the generative procedure will stop almost everywhere on the space Ω. Under the same condition,

using a similar argument as in Theorem 2 in Wong and Ma (2010), one can show that with probability 1 this procedure will produce a pair of well-defined probability measures (Q_1, Q_2) that are both absolutely continuous with respect to the baseline measure Q_0. Thus, we can formally define this generative model as a distribution on a pair of probability measures.

Definition 1. *The pair of random probability measures (Q_1, Q_2) is said to have a divide-merge Markov tree (DMMT) distribution with parameters $\boldsymbol{\rho}, \boldsymbol{\alpha}, \boldsymbol{\lambda}$,and baseline measure Q_0. We write $(Q_1, Q_2) \sim DMMT(\boldsymbol{\rho}, \boldsymbol{\alpha}, \boldsymbol{\lambda}, Q_0)$.*

The next theorem shows that the DMMT has large L_1 support, and thus can be used as a nonparametric prior.

Theorem 1. *Assume $(Q_1, Q_2) \sim DMMT(\boldsymbol{\rho}, \boldsymbol{\alpha}, \boldsymbol{\lambda}, Q_0)$ where*

1. *The initial state $\rho_{0,s} < 1$.*
2. *The transition probabilities $\rho_{d,d}(A), \rho_{d,m}(A), \rho_{d,s}(A), \rho_{m,m}(A), \rho_{m,s}(A)$, the direction probabilities $\lambda_j(A, g)$ and the pseudo-count parameters $\alpha_t(A_l^j, g)/(\alpha_t(A_l^j, g) + \alpha_t(A_r^j, g))$ are uniformly bounded away from 0 and 1, for all $A \in \mathcal{A}^{(\infty)}$ and $g \in \{d, m\}$.*

Then, for any pair of distributions F_1 and F_2 absolutely continuous w.r.t. Q_0 and any $\tau > 0$, we have

$$\Pr\Big(\int |\tilde{q}_t - \tilde{f}_t| dQ_0 < \tau, \ \textit{for } t = 1, 2\Big) > 0,$$

where $\tilde{q}_t = dQ_t/dQ_0$ and $\tilde{f}_t = dF_t/dQ_0$.

Proof. See Supplementary Material. □

One can center a DMMT distribution at the baseline measure Q_0. More specifically, if $\text{DMMT}(\boldsymbol{\rho}, \boldsymbol{\alpha}, \boldsymbol{\lambda}, Q_0)$ satisfies:

1. There exists a $\delta > 0$ such that $\rho_{g,s}(A) > \delta$ for all $A \in \mathcal{A}^{(\infty)}$ and $g \in \mathcal{G}$;

2. For all $A \in \mathcal{A}^{(\infty)}$ such that $Q_0(A) > 0$, $j = 1, \ldots p$ and $g \in \{d, m\}$:

$$\frac{\alpha^j_{t,l}(A, g)}{\alpha^j_{t,l}(A, g) + \alpha^j_{t,r}(A, g)} = \frac{Q_0(A^j_l)}{Q_0(A)}, \tag{1}$$

then $E(Q_t(B)) = Q_0(B)$ for any $B \in \mathcal{B}(\Omega)$ and $E(q_t(x)) = q_0(x)$, where $t = 1, 2$, $q_t = dQ_t/d\mu$ and $q_0 = dQ_0/d\mu$ with μ being a dominating measure such as the Lebesgue measure. We shall refer to condition (1) as the centering condition.

In some situations, we have a general idea of the common shape of the two distributions, and are able to elicit it with a simple distribution from a given parametric family. In this case, one can center the DMMT prior at a given Q_0 that reflects this prior knowledge. This helps to achieve parsimony, allowing the process to focus on modeling the differential structure between the two distributions, and thus yielding increased power in two-sample comparison.

2.3 The posterior of a DMMT prior

In this section we find the corresponding posterior of a DMMT prior. Later we will use the posterior to carry out inferential tasks such as two-sample comparison in a Bayesian paradigm. Our main result (Theorem 2) shows that the DMMT process is posterior conjugate, in the sense that if (Q_1, Q_2) has a DMMT prior, then after observing i.i.d. data samples from Q_1 and Q_2, the posterior is still a DMMT distribution. Moreover, the posterior parameters can be computed recursively. This intriguing result follows from the Markov nature of the DMMT process, and the results in this section correspond to a "forward-summation-backward-sampling" algorithm for computing posterior Markov models (Liu, 2008). More specifically, Lemma 1 corresponds to the "forward-summation" step for the DMMT process while Theorem 2 the "backward-sampling" step. Lemma 2 shows that the recursion can be carried out analytically even when the partition sequence is infinite. Readers less interested in the technical details may directly jump to those results.

Assume that $(Q_1, Q_2) \sim \text{DMMT}(\boldsymbol{\rho}, \boldsymbol{\alpha}, \boldsymbol{\lambda}, Q_0)$, and we observe two groups of i.i.d. samples $\boldsymbol{x}_1 = (x_{1,1}, \ldots, x_{1,n_1})$ and $\boldsymbol{x}_2 = (x_{2,1}, \ldots, x_{2,n_2})$ on Ω from Q_1 and Q_2, respectively. In the following, we shall use $\boldsymbol{x}_1 \cup \boldsymbol{x}_2$ to represent the pooled sample $(x_{1,1}, \ldots, x_{1,n_1}, x_{2,1}, \ldots, x_{2,n_2})$. Let $q_t(x|A) = q_t(x)/Q_t(A)$ for $x \in A$ be the conditional density on A of Q_t for $t = 0, 1, 2$. Then, the conditional likelihood on A is

$$q(\boldsymbol{x}_1, \boldsymbol{x}_2|A) = \prod_{t=1,2} q_t(\boldsymbol{x}_t|A), \tag{2}$$

where $q_t(\boldsymbol{x}_t|A) = \prod_{x_{t,j} \in A} q_t(x_{t,j}|A)$ for $t = 1, 2$. We introduce a mapping $\Phi : \mathcal{A}^{(\infty)} \times \mathcal{G} \times \Omega^{n_1} \times \Omega^{n_2} \mapsto \mathbb{R}$, which will be useful in expressing the posterior of a DMMT,

$$\Phi(A, g, \boldsymbol{x}_1, \boldsymbol{x}_2) := \int q(\boldsymbol{x}_1, \boldsymbol{x}_2|A)\pi(dQ_1, dQ_2|E_1(A), E_{2,g}(A)), \tag{3}$$

where $\pi(\cdot, \cdot)$ denotes the prior of (Q_1, Q_2), $E_1(A) = \{A \text{ arises during the random partitioning}\}$ and $E_{2,g}(A) = \{S(\text{parent}(A)) = g\}$ and $g \in \mathcal{G}$. This quantity represents the conditional likelihood on A integrated with respect to the prior on (Q_1, Q_2), given that the parent of A is in state g and A arises during the random partitioning. Notice that the DMMT process restricted on A is still a DMMT on A due to its self-similarity, thus (3) represents the marginal likelihood for a DMMT with root being A and initial state $\rho_{0,g} = 1$. Lemma 1 provides a recursive representation of (3).

Lemma 1. *For every $A \in \mathcal{A}^{(\infty)}$ and $g \in \mathcal{G}$, $\Phi(A, g, \boldsymbol{x}_1, \boldsymbol{x}_2)$ has the following recursive representation*

$$\Phi(A, g, \boldsymbol{x}_1, \boldsymbol{x}_2) = \sum_{h \in \mathcal{G}} \rho_{g,h}(A) Z(A, h, \boldsymbol{x}_1, \boldsymbol{x}_2),$$

where

$$Z(A, g, \boldsymbol{x}_1, \boldsymbol{x}_2) = \begin{cases} \sum_{j=1}^{p} Z_j(A, g, \boldsymbol{x}_1, \boldsymbol{x}_2) & \text{if } g \in \{d, m\} \\ \prod\limits_{x \in \boldsymbol{x}_1 \cup \boldsymbol{x}_2} q_0(x|A) & \text{if } g = s, \end{cases}$$

$$Z_j(A, g, \boldsymbol{x}_1, \boldsymbol{x}_2) = \begin{cases} \lambda_j(A, m) \dfrac{D(\boldsymbol{\alpha}^j(A, m) + \boldsymbol{n}_1^j(A) + \boldsymbol{n}_2^j(A))}{D(\boldsymbol{\alpha}^j(A, m))} \prod\limits_{i \in \{l, r\}} \Phi(A_i^j, m, \boldsymbol{x}_1, \boldsymbol{x}_2) & \text{if } g = m \\ \lambda_j(A, d) \prod\limits_{t=1,2} \dfrac{D(\boldsymbol{\alpha}_t^j(A, d) + \boldsymbol{n}_t^j(A))}{D(\boldsymbol{\alpha}_t^j(A, d))} \prod\limits_{i \in \{l, r\}} \Phi(A_i^j, d, \boldsymbol{x}_1, \boldsymbol{x}_2) & \text{if } g = d, \end{cases}$$

for $j = 1, \ldots, p$, $t = 1, 2$, $\boldsymbol{n}_t^j(A) = \big(n_t(A_l^j), n_t(A_r^j)\big)$, $n_t(A) = |\{x_{t,i} : x_{t,i} \in A, \ i = 1, 2, \ldots, n_t\}|$ *and* $D(w_1, w_2) = \Gamma(w_1)\Gamma(w_2)/\Gamma(w_1 + w_2)$.

Proof. See Supplementary Material. □

This representation of Φ is recursive in its first argument in the sense that one can compute $\Phi(A, \cdot, \cdot, \cdot)$ based on $\Phi(A_i^j, \cdot, \cdot, \cdot)$. This recursive representation becomes operational if (3) can be eventually expressed in closed form. Lemma 2 provides analytic expressions for some specific regions.

Lemma 2. *For two types of regions* $\Phi(A, g, \boldsymbol{x}_1, \boldsymbol{x}_2)$ *is known analytically:*

1. *Empty regions, i.e.* $A : (\boldsymbol{x}_1 \cup \boldsymbol{x}_2) \cap A = \emptyset$, *then* $\Phi(A, g, \boldsymbol{x}_1, \boldsymbol{x}_2) = 1$;
2. *Regions with a single observation, i.e.* $A : |(\boldsymbol{x}_1 \cup \boldsymbol{x}_2) \cap A| = 1$, *then* $\Phi(A, g, \boldsymbol{x}_1, \boldsymbol{x}_2) = \prod_{x \in \boldsymbol{x}_1 \cup \boldsymbol{x}_2} q_0(x|A)$ *under the centering condition.*

Proof. See Supplementary Material. □

For every finite sample size $n_1 + n_2$, there is a finite partitioning level k such that all the nodes of level k in the partitioning tree belong to one of these two types of "terminal" nodes. Thus, (3) can be computed recursively from these nodes of the tree up to the root. Finally, Theorem 2 establishes the conjugacy of DMMT and provides expression for the posterior parameters.

Theorem 2. *Suppose we observe two groups of i.i.d. samples* $\boldsymbol{x_1} = (x_{1,1}, \ldots, x_{1,n_1})$ *and* $\boldsymbol{x_2} = (x_{2,1}, \ldots, x_{2,n_2})$ *from two distributions* Q_1 *and* Q_2*. If* (Q_1, Q_2) *have a DMMT*$(\boldsymbol{\rho}, \boldsymbol{\lambda}, \boldsymbol{\alpha}, Q_0)$ *prior, then, the posterior of* (Q_1, Q_2) *is still a DMMT with the same baseline* Q_0 *and the following parameters:*

1. *Transition probabilities:*

$$\rho_{g,h}(A|\boldsymbol{x}_1, \boldsymbol{x}_2) = \rho_{g,h}(A)\frac{Z(A, h, \boldsymbol{x}_1, \boldsymbol{x}_2)}{\Phi(A, g, \boldsymbol{x}_1, \boldsymbol{x}_2)} \quad \textit{for all } A \in \mathcal{A}^{(\infty)}, g, h \in \mathcal{G}.$$

2. *Direction probabilities:*

$$\lambda_j(A, g|\boldsymbol{x}_1, \boldsymbol{x}_2) = \frac{Z_j(A, g, \boldsymbol{x}_1, \boldsymbol{x}_2)}{Z(A, g, \boldsymbol{x}_1, \boldsymbol{x}_2)} \quad \textit{for all } A \in \mathcal{A}^{(\infty)}, g \in \{d, m\} \textit{ and } j = 1, \ldots, p.$$

3. *Pseudo-counts:*

$$\alpha_t(A, g|\boldsymbol{x}_1, \boldsymbol{x}_2) = \begin{cases} \alpha_t(A, d) + n_t(A) & \textit{if } g = d \\ \alpha_t(A, m) + n_1(A) + n_2(A) & \textit{if } g = m, \end{cases}$$

for all $A \in \mathcal{A}^{(\infty)}$ *and* $t = 1, 2$.

Proof. See Supplementary Material. □

2.4 Two-sample testing

Two probability measures (Q_1, Q_2) with a DMMT distribution are identical if and only if the DMMT process, in any part of the partition tree, is never in the divide state. The posterior probability of this event, H_0, is given by

$$\Pr(H_0|\boldsymbol{x}_1, \boldsymbol{x}_2) = \int 1\left(Q_1(\cdot) = Q_2(\cdot)\right) \pi(dQ_1, dQ_2|\boldsymbol{x}_1, \boldsymbol{x}_2), \tag{4}$$

where $\pi(\cdot,\cdot|\boldsymbol{x}_1,\boldsymbol{x}_2)$ denotes the posterior DMMT. This probability can be estimated by drawing samples of the two distributions from the posterior, and computing the proportion of draws that are never in the divide state, i.e.,

$$\frac{1}{B}\sum_{b=1}^{B} 1\left(Q_1^{(b)}(\cdot) = Q_2^{(b)}(\cdot)\right), \quad \text{where } \left(Q_1^{(b)}, Q_2^{(b)}\right) \sim (Q_1, Q_2)|\boldsymbol{x}_1, \boldsymbol{x}_2.$$

Alternatively, again due to the Markov nature of the DMMT, one can evaluate $\Pr(H_0|\boldsymbol{x}_1,\boldsymbol{x}_2)$ analytically through another "forward-summation" type recursion, eliminating the Monte Carlo error involved in posterior sampling. To see this, we define another mapping $\Psi : \mathcal{A}^{(\infty)} \times \mathcal{G} \times \Omega^{n_1} \times \Omega^{n_2} \mapsto [0,1]$.

$$\Psi(A, g, \boldsymbol{x}_1, \boldsymbol{x}_2) = \int 1\left(Q_1(\cdot|A) = Q_2(\cdot|A)\right) \pi(dQ_1, dQ_2|\boldsymbol{x}_1, \boldsymbol{x}_2, E_1(A), E_{2,g}(A)).$$

This function represents the marginal posterior probability that the two distributions are identical conditional on A, given that A arises as a node in the partition tree and the process is in state g on the parent of A.

Lemma 3. *The mapping $\Psi(A, g, \boldsymbol{x}_1, \boldsymbol{x}_2)$ has the following recursive representation*

$$\begin{aligned}\Psi(A, g, \boldsymbol{x}_1, \boldsymbol{x}_2) = \rho_{g,s}(A|\boldsymbol{x}_1, \boldsymbol{x}_2) \\ + \rho_{g,m}(A|\boldsymbol{x}_1, \boldsymbol{x}_2) \sum_{j=1}^{p} \lambda_j(A, m|\boldsymbol{x}_1, \boldsymbol{x}_2) \prod_{i\in\{l,r\}} \Psi(A_i^j, m, \boldsymbol{x}_1, \boldsymbol{x}_2), \quad (5)\end{aligned}$$

for all $A \in \mathcal{A}^{(\infty)}$ and $g \in \mathcal{G}$.

Proof. See Supplementary Material. □

For $g = s$, $\Psi(A, g, \boldsymbol{x}_1, \boldsymbol{x}_2) = 1$, since $\rho_{g,s}(A|\boldsymbol{x}_1, \boldsymbol{x}_2) = \rho_{g,s}(A) = 1$. For all other regions and states, it can be evaluated with arbitrary precision by terminating the recursive at a deep

enough finite level because $0 \leq \Psi(A, g, \boldsymbol{x}_1, \boldsymbol{x}_2) \leq 1$ for all $A \in \mathcal{A}^{(\infty)}$ and $g \in \mathcal{G}$. In particular, we can compute $\Psi(\Omega, g, \boldsymbol{x}_1, \boldsymbol{x}_2)$ with arbitrary precision. Now we can formally describe how the posterior probability that the two distributions are identical can be computed.

Proposition 1. *Suppose we observe two groups of i.i.d. samples* $\boldsymbol{x}_1 = (x_{1,1}, \ldots, x_{1,n_1})$ *and* $\boldsymbol{x}_2 = (x_{2,1}, \ldots, x_{2,n_2})$ *from two distributions* Q_1 *and* Q_2*. Let* (Q_1, Q_2) *have a DMMT*$(\boldsymbol{\rho}, \boldsymbol{\lambda}, \boldsymbol{\alpha}, Q_0)$ *prior. Then the posterior probability that the two distributions are identical is given by*

$$\Pr(H_0|\boldsymbol{x}_1, \boldsymbol{x}_2) = \sum_{g \in \mathcal{G}} \rho_{0,g} \Psi(\Omega, g, \boldsymbol{x}_1, \boldsymbol{x}_2).$$

Proof. See Supplementary Material. □

The next two theorems establish the consistency for the two-sample test using DMMT.

Theorem 3. (Consistency under the alternative) *We observe two independent groups of i.i.d. samples* $\boldsymbol{x_1} = (x_{1,1}, \ldots, x_{1,n_1})$ *and* $\boldsymbol{x_2} = (x_{2,1}, \ldots, x_{2,n_2})$ *from two distributions* Q_1 *and* Q_2*, where* $n = n_1 + n_2 \to \infty$*, and* $n_1/n \to \beta$ *for some* $\beta \in (0, 1)$*. Let* (Q_1, Q_2) *have a DMMT*$(\boldsymbol{\rho}, \boldsymbol{\lambda}, \boldsymbol{\alpha}, Q_0)$ *prior where the conditions of Theorem 1 and the centering condition are satisfied. In addition, if* $\rho_{d,g}(A) \in (0, 1)$ *for all* $g \in \mathcal{G}$ *and* $A \in \mathcal{A}^{(k)}$ *for some large enough* k*, then,*

$$\Pr(H_0|\boldsymbol{x}_1, \boldsymbol{x}_2) \xrightarrow{p} 0 \text{ under } P_1^{(\infty)} \times P_2^{(\infty)},$$

for $P_1 \ll Q_0$ *and* $P_2 \ll Q_0$ *provided that there exists* $A \in \mathcal{A}^{(\infty)}$ *such that* $P_1(A_i^j|A) \neq P_2(A_i^j|A)$ *and* $\beta P_1(A_i^j|A) + (1 - \beta) P_2(A_i^j|A) \neq Q_0(A_i^j|A)$ *for some* $j = 1, \ldots, p$ *and* $i = l, r$*.*

Proof. See the Supplementary Material. □

Theorem 4. (Consistency under the null) *We observe two independent groups of i.i.d. samples* $\boldsymbol{x_1} = (x_{1,1}, \ldots, x_{1,n_1})$ *and* $\boldsymbol{x_2} = (x_{2,1}, \ldots, x_{2,n_2})$ *from two distributions* Q_1 *and* Q_2*, where* $n = n_1 + n_2 \to \infty$*, and* $n_1/n \to \beta$ *for some* $\beta \in (0, 1)$*. Let* (Q_1, Q_2) *have*

a DMMT$(\boldsymbol{\rho}, \boldsymbol{\lambda}, \boldsymbol{\alpha}, Q_0)$ *prior where the centering condition are satisfied. In addition, if for some* $k \in \mathbb{N}$

1. $\rho_{g,h}(A) \in (0,1)$ *for all* $g \in \mathcal{G}$, $h \in \{d, m\}$ *and* $A \in \mathcal{A}^{(k)}$.

2. $\rho_{g,d}(A) = 0$ *for all* $g \in \mathcal{G}$, $A \in \mathcal{A}^l$ *and for all* $l > k$,

then,

$$\Pr(H_0|\boldsymbol{x}_1, \boldsymbol{x}_2) \xrightarrow{p} 1 \text{ under } P_0^{(\infty)} \times P_0^{(\infty)} \text{ for any } P_0 \ll Q_0.$$

Proof. See the Supplementary Material. □

2.5 Identifying the differential structure

In many applications it is important not only to test two-sample difference, but to identify the differential structure. The multi-resolution approach provides a natural means to identifying differences through specifying the location, scale, and effect size of the difference. All such information is encapsulated in the full DMMT posterior and can be extracted through posterior Monte Carlo sampling or constructing summaries of the posterior. Here we design a strategy for effectively summarizing such posterior information. This is particularly useful when one is interested in learning the general structure of the difference rather than checking specific aspects of the difference that one has in mind. (The latter task is more readily achieved through Monte Carlo sampling.)

Our strategy is first identify a representative partition tree that effectively characterizes the two-sample difference and then report all regions in this tree that are *a posteriori* very likely to be in the divide state. Our representative partition tree is determined using two types of posterior summaries that respectively shed light on how to further partition a tree node and when to stop the partitioning. More specifically, we summarize the posterior information regarding how to further partition a tree node using the posterior direction

probabilities weighted accordingly to the marginal posterior probability of each non-stopping state

$$\lambda_j^*(A|\boldsymbol{x}_1, \boldsymbol{x}_2) = \sum_{g \in \{d,m\}} \rho_g^*(A|\boldsymbol{x}_1, \boldsymbol{x}_2)\lambda_j(A, g|\boldsymbol{x}_1, \boldsymbol{x}_2),$$

where $A \in \mathcal{A}^{(\infty)}$, $j = 1, \ldots, p$. The summary for determining whether to stop further partitioning is

$$\rho_g^*(A|\boldsymbol{x}_1, \boldsymbol{x}_2) = P\big(S(A) = g|\boldsymbol{x}_1, \boldsymbol{x}_2, B(A)\big) \quad \text{for } g \in \mathcal{G}, \tag{6}$$

where $B(A)$ is the collection of ancestral sets of A in the partition tree, i.e. the branch of the partition tree that extends from Ω to A. This probability is marginalized over the hidden states along this branch. It can be computed recursively:

$$\rho_g^*(A|\boldsymbol{x}_1, \boldsymbol{x}_2) = \begin{cases} \sum_{h \in \mathcal{G}} \rho_{0,h}\rho_{h,g}(A|\boldsymbol{x}_1, \boldsymbol{x}_2) & \text{if } A = \Omega \\ \sum_{h \in \mathcal{G}} \rho_h^*(\text{parent}(A)|\boldsymbol{x}_1, \boldsymbol{x}_2)\rho_{h,g}(A|\boldsymbol{x}_1, \boldsymbol{x}_2) & \text{if } A \in \mathcal{A}^{(\infty)} \setminus \{\Omega\}, \end{cases}$$

for all $g \in \mathcal{G}$.

Based on these two types of summaries, the representative tree is constructed using the following top-down sequential procedure. Starting from the root $A = \Omega$, if $\rho_s^*(A|\boldsymbol{x}_1, \boldsymbol{x}_2) > 1 - \delta^*$ for some threshold $\delta^* \in (0, 1)$, then we stop; otherwise we divide the tree in the direction j that maximizes $\lambda_j^*(A|\boldsymbol{x}_1, \boldsymbol{x}_2)$. For each A_i^j we repeat this procedure until all branches are stopped.

Additionally, we define a notion of *effect size* to summarize the extent to which the two distributions are different on each reported region. The *effect size* on A is given by

$$\text{Eff}(A|\boldsymbol{x}_1, \boldsymbol{x}_2) = \max_{j=1,\ldots,p} \left| \log \frac{\alpha_1(A_l^j, d|\boldsymbol{x}_1, \boldsymbol{x}_2)/\alpha_1(A_r^j, d|\boldsymbol{x}_1, \boldsymbol{x}_2)}{\alpha_2(A_l^j, d|\boldsymbol{x}_1, \boldsymbol{x}_2)/\alpha_2(A_r^j, d|\boldsymbol{x}_2, \boldsymbol{x}_2)} \right|. \tag{7}$$

This quantity is large when the proportion of probability mass in the two children regions

A_l^j, A_r^j is very different between the two groups for at least one of the p dimensions.

2.6 Prior specification and spatial clustering of differences

The number of parameters characterizing the DMMT process is infinite, but structural and symmetric assumptions on the prior parameters can substantially simplify the specification of the prior. In this section we suggest default choices for these parameters.

A simple and reasonable choice for the prior transition matrix $\boldsymbol{\rho}(A)$ is to make it dependent on the level of the A, .i.e., $\boldsymbol{\rho}(A) = \boldsymbol{\rho}(k)$. Additionally, we adopt a parsimonious and yet flexible functional form to further reduce the elicitation of the prior to a small number of parameters. More specifically, we define

$$\boldsymbol{\rho}(k) = \begin{bmatrix} \beta & (1-\beta)/2 & (1-\beta)/2 \\ \gamma 2^{-k} & (1-\gamma 2^{-k})/2 & (1-\gamma 2^{-k})/2 \\ 0 & 0 & 1 \end{bmatrix},$$

for some $\beta, \gamma \in (0,1)$. The parameter β determines the spatial clustering of the differential structure. Given a set on which the process is in the divide state, a larger β will suggest a higher likelihood of children and neighbors also being in the divide state. The parameter γ controls the transition from the merge state to the divide state, and the 2^{-k} factor is included to provide adequate control for multiple testing. The number of sets in $\mathcal{A}^k$ increases geometrically in the depth k, and the 2^{-k} factor ensures that the prior probabilities of the divide state decrease accordingly.

The parameters β and γ along with the initial state probabilities controls the prior marginal null probability that the two distributions are identical. Because the stop state is irreversible, one should fix $\rho_{0,s} = 0$. This leaves three free parameters β, γ, and $\rho_{0,d}$ to be specified. A useful strategy to choosing these parameters is to set the prior marginal null

probability to some moderate value such as 0.5. Simple choices such as $\beta = 0.3$, $\gamma = 0.2$ and $\rho_{0,d} = 1$ that satisfy this constraint are highly effective in a variety of numerical examples. A sensitivity analysis shows that the posterior inference is robust to the prior specification. The results of the analysis are reported in the Supplementary Material.

Without prior knowledge about what dimensions are more likely to be involved in characterizing the two distributions, a natural noninformative choice for the direction probabilities is $\lambda_j(A, g) = 1/p$ for $j = 1, \ldots, p$, and $g \in \{d, m\}$. Finally, a standard noninformative choice for the pseudo-counts is $\alpha^j_{t,l}(A, g) = Q_0(A^j_l)/Q_0(A)$ and $\alpha^j_{t,r}(A, g) = Q_0(A^j_r)/Q_0(A)$, respecting the centering condition.

3 Numerical examples

In this section we provide three numerical examples. The first two are simulated and the last a real flow cytometry data set. We compare the performance of DMMT for two-sample testing—using $\Pr(H_0|\boldsymbol{x}_1, \boldsymbol{x}_2)$ as a test statistic—to those of several other state-of-the-art methods. We then illustrate how to identify and summarize differential structures using the strategy given in Section 2.5. The dimensionalities of the three examples are one, two and seven. For all these examples, we use a uniform baseline and follow the general recipe for prior specification given in Section 2.6. In particular, we set $\beta = 0.3$, $\gamma = 0.2$ and $\rho_{0,d} = 1$, and we let $\rho_{g,s}(k) = 1$ for level $k = 12$. To identify the differential structure we consider the representative partition tree with $\delta^* = 0.8$. We use the range of the data points in each dimension to define the hyper-rectangle Ω.

3.1 Example 1

In Example 1 we consider the following two-sample problems in $\mathbb{R}$. For each problem we generate 1,000 datasets, and for each dataset we construct a corresponding "null" dataset

by randomly permuting the labels of the two groups.

1. Local shift difference ($n_1 = n_2 = 200$): $X_1 \sim 0.9\mathcal{N}(0.2, 0.05^2) + 0.1\mathcal{N}(0.9, 0.01^2)$, $X_2 \sim 0.9\mathcal{N}(0.2, 0.05^2) + 0.1\mathcal{N}(0.88, 0.01^2)$.

2. Local dispersion difference ($n_1 = n_2 = 200$): $X_1 \sim 0.9\mathcal{N}(0.2, 0.05^2) + 0.1\mathcal{N}(0.8, 0.01^2)$, $X_2 \sim 0.9\mathcal{N}(0.2, 0.05^2) + 0.1\mathcal{N}(0.8, 0.04^2)$.

3. Global shift difference ($n_1 = n_2 = 100$): $X_1 \sim \mathcal{N}(-0.5, 2^2), \quad X_2 \sim \mathcal{N}(0.5, 2^2)$.

4. Global dispersion difference ($n_1 = n_2 = 50$): $X_1 \sim \mathcal{N}(0, 1^2), \quad X_2 \sim \mathcal{N}(0, 2^2)$.

In the first row of Figure 2 we plot the pair of density functions for each scenario. In the first two scenarios the difference is located in a small region of the sample, while in the last two the difference is global. In the second row of Figure 2 we compare the ROC curves of five different statistics for testing the hypothesis that the two distributions are identical. The other four test statistics are the k-nearest neighbors test (KNN) (Schilling (1986), and Henze (1988)), the Cramér test (Baringhaus and Franz, 2004), co-OPT (Ma and Wong, 2011) and Holmes et al. (2012)'s PT Bayes factor. We use the R package `MTSKNN` (Chen et al., 2010) for the KNN test and the R package `cramer` (Franz, 2006) for the Cramér test.

The DMMT outperforms the other methods in the local difference scenarios and behaves well in the global difference ones. KNN behaves well in the local difference scenarios, but is not efficient in the global scenarios. Cramér, instead, is good in testing larger-scale differences, but performs extremely poorly for local differences.

In Figure 3 we illustrate how to identify differences at multiple resolution levels using the posterior representative partition tree for the local shift difference scenario. On the left plot we use a blue-scale to represent the marginal posterior probability of the divide state $\rho_d^*(\cdot|\boldsymbol{x}_1, \boldsymbol{x}_2)$ on each node; while on the right plot, we use a red-scale to visualize the effect

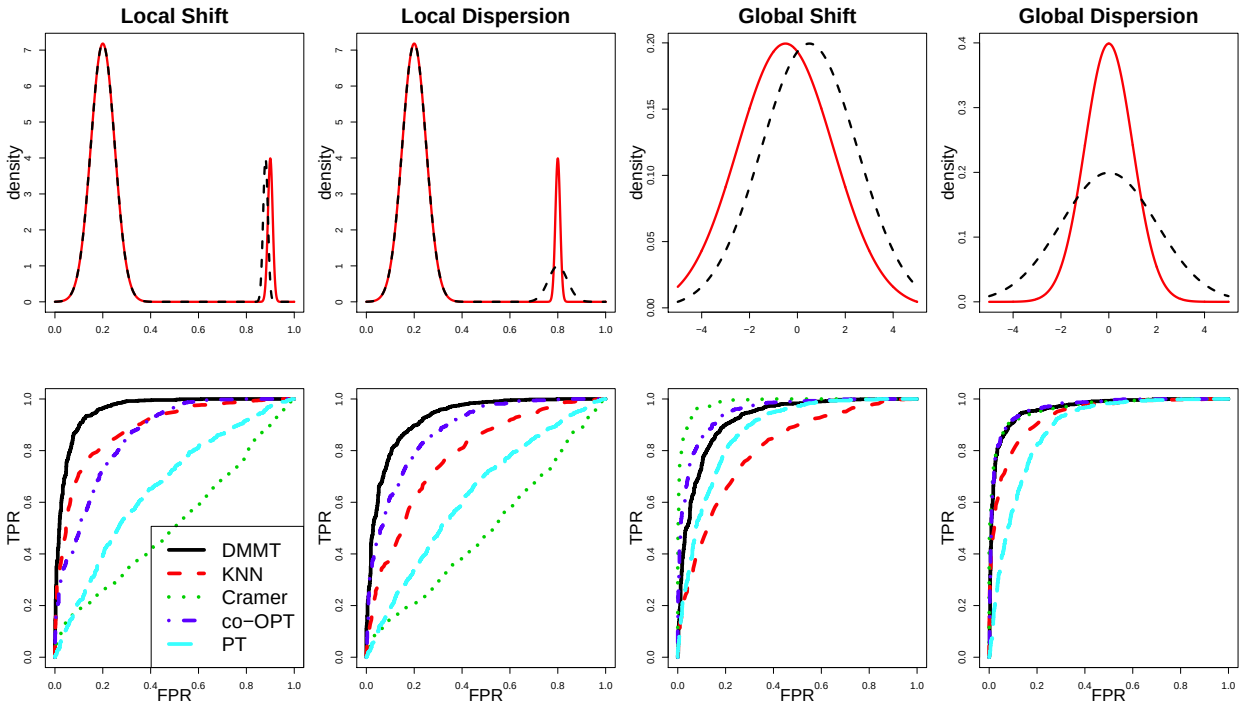

Figure 2: Two-sample problems in $\mathbb{R}$. First row: densities of the two distributions under the different scenarios - Sample 1 red solid; Sample 2 black dashed. Second row: the ROC curves for each of the testing method considered - DMMT black solid; KNN red dash; Cramér green dotted; co-OPT blue dotted dash; PT pale blue long dash.

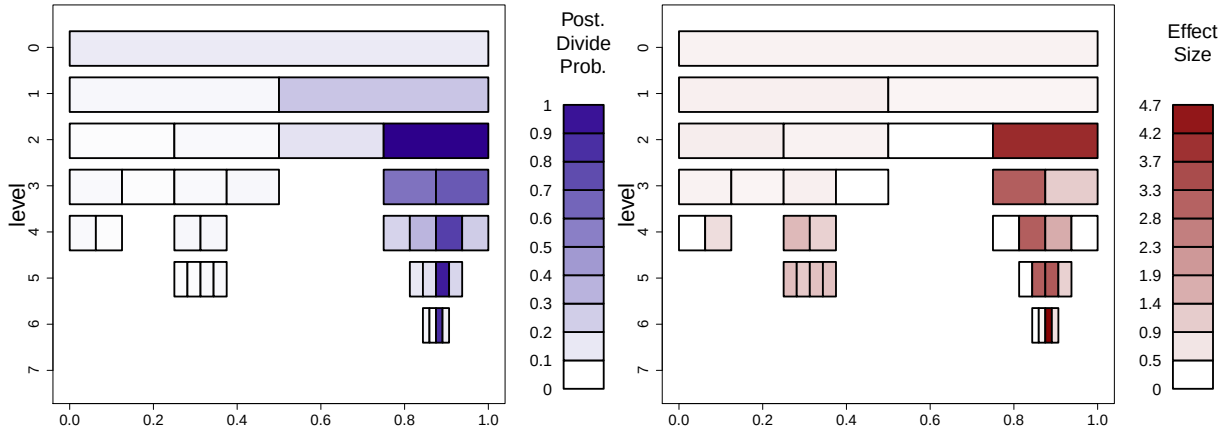

Figure 3: Nested sequence of partitions for the local shift difference scenario in $\mathbb{R}^1$. On the left, for each region the dark/light blue represents high/low posterior probability of being on the divide state. On the right, for each region the dark/light red represents high/low effect size.

size. The two distributions share the same normal component on the left, while the difference is located on the right, which is effectively captured in the posterior summary. The spatial clustering of the difference is also reflected in the patch of dark blue and red in the lower right corner of the two plots.

In the Supplementary Material we provide an analysis of sensitivity to the prior choice, showing that the results are robust to the prior specification. Similar results are obtained for the other scenarios and examples and so are not reported.

3.2 Example 2

We consider the following two-sample problems in $\mathbb{R}^2$. For each problem we again generate 1,000 datasets, and for each dataset we construct a corresponding "null" dataset by randomly permuting the labels of the two groups.

1. Local shift difference ($n_1 = n_2 = 400$): $X_1 \sim p_1\mathcal{N}_2(\mu_1, \Sigma_1) + \sum_{k=2}^{5} p_k\mathcal{N}_2(\mu_k, \Sigma_k)$, $X_2 \sim p_1\mathcal{N}_2(\mu_1 + \delta, \Sigma_1) + \sum_{k=2}^{5} p_k\mathcal{N}_2(\mu_k, \Sigma_k)$, where $\delta = (1, 1)$, while p_k, μ_k and Σ_k are provided in Appendix A.

2. Local dispersion difference ($n_1 = n_2 = 400$): $X_1 \sim p_1\mathcal{N}_2(\mu_1, \Sigma_1) + \sum_{k=2}^{5} p_k\mathcal{N}_2(\mu_k, \Sigma_k)$, $X_2 \sim p_1\mathcal{N}_2(\mu_1, 5\Sigma_1) + \sum_{k=2}^{5} p_k\mathcal{N}_2(\mu_k, \Sigma_k)$, where p_k, μ_k and Σ_k are provided in Appendix A.

3. Global shift difference ($n_1 = n_2 = 100$): $X_1 \sim \mathcal{N}_2(0, \Sigma)$, $\quad X_2 \sim \mathcal{N}_2(\delta, \Sigma)$, where $\delta = (1, 0)$, while Σ is provided in Appendix A.

4. Global dispersion difference ($n_1 = n_2 = 50$): $X_1 \sim \mathcal{N}_2(0, I_2)$, $\quad X_2 \sim \mathcal{N}_2(0, 3I_2)$.

In Figure 4 we plot the ROC curve for DMMT and the other methods. The results are similar to what we have obtained in the 1D example. The performance of DMMT dominates two of the competing methods—KNN and PT—in the sense that DMMT is at least as good in

all four scenarios. The performance gain over the co-OPT is largely due to incorporation of spatial clustering through Markov dependence, while the gain over the PT is due to both the Markov dependence and the data-adaptive partition sequence. On the other hand, DMMT does substantially better than Cramér for local differences, while Cramér is more powerful, though to a lesser extent, for the global differences.

For a typical data set in the local shift difference scenario, we again illustrate how to identify the differential structure. We plot in Figure 5 the representative partition tree. For each region, we show the marginal posterior probability of the divide state $\rho_d^*(\cdot|\boldsymbol{x}_1, \boldsymbol{x}_2)$. These regions correctly identify the local differences between the two distributions.

3.3 A 7-dimensional flow cytometry dataset

Flow cytometry is a popular laser technology for measuring the protein levels of single cells on thousands of cells. In this example we have two blood samples from the same patient, where each sample contains over $300,000$ cells, and for each cell the following 7 markers are measured: FSC-A, FSC-H, SSC-A, Dext, CD4, CD8 and Aqua. In one of the two samples some cells have been transfected via electroporation with a T cell receptor gene specific for Tyrosinase (see Singh et al. (2013) for further details). The dexter conjugated with a fluorescent dye detects Tyrosinase-spefic CD8 T cell receptors, and a higher concentration of transfected cells is expected in the population of cells that are both CD8 and Dext high.

The primary goal of this analysis is to identify cell subpopulations that differentiate the two cell samples. For this reason the existing two sample tests such as KNN and Cramér are not useful here as one cannot pinpoint the difference with the tests.

We apply our DMMT process to model the underlying distributions. The posterior probability for the two samples to be equal is virtually 0. Using the representative partition tree we identify several differential regions with significant two-sample differences. In Figure 6 we plot five 2-dimensional projections of the data, highlighting in yellow the differential

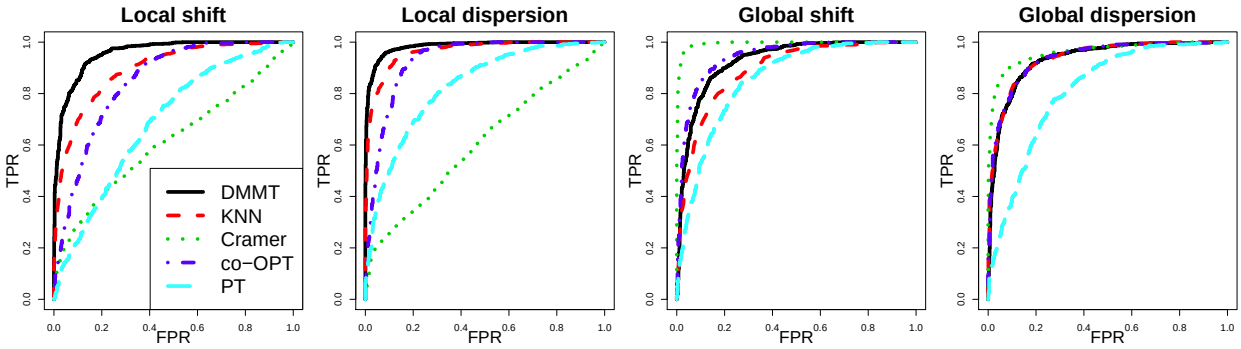

Figure 4: Two-sample problems in $\mathbb{R}^2$. ROC curves for each of the testing method considered - DMMT black solid; KNN red dash; Cramér green dotted; co-OPT blue dotted dash; PT pale blue long dash.

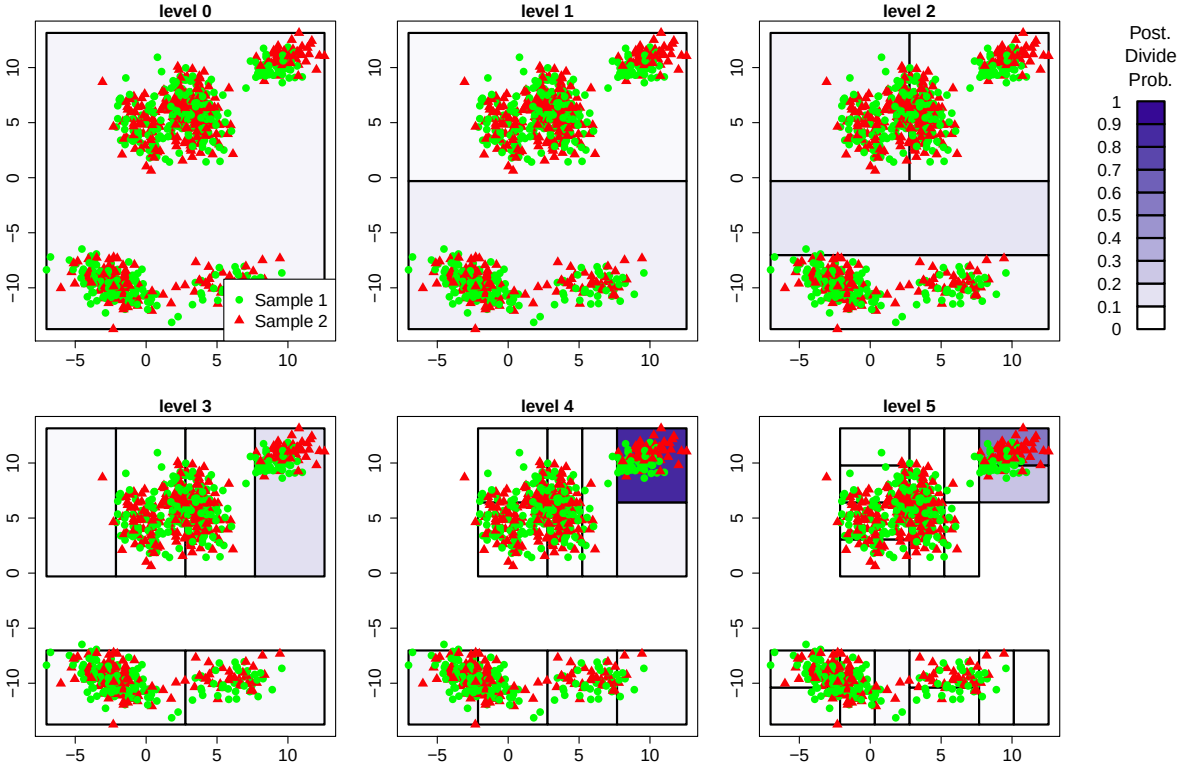

Figure 5: The representative partition tree for a draw from the local shift difference scenario in $\mathbb{R}^2$. Sample 1 green dots; Sample 2 red triangles. For each region the dark/light blue represents high/low posterior probability of being on the divide state.

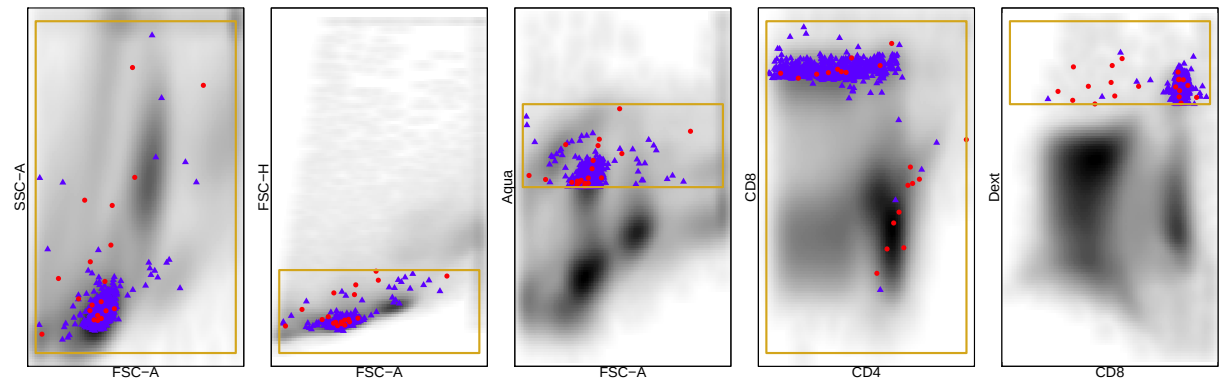

Figure 6: Five projections of the flow cytometry dataset. For each projection the yellow rectangle highlights the differential region with the largest effect size among the regions with $\rho_d^*(\cdot|\boldsymbol{x}_1, \boldsymbol{x}_2) > \delta^*$. The red dots and the blue triangles represent respectively the normal and transfected cells within the differential region. In the plot on the far right we observe a cluster of transfected cells (blue triangles).

region with the largest effect size among the regions with $\rho_d^*(\cdot|\boldsymbol{x}_1, \boldsymbol{x}_2) > \delta^*$. In particular, $\rho_d^*(\cdot|\boldsymbol{x}_1, \boldsymbol{x}_2) = 0.998$ and the effect size is 4.35. We "smeared" out the cells that do not fall into our detected region. The volume of the region is 1/64 of the entire sample space and contains respectively 0.006% and 0.220% of the two cell populations (indicated with red dots and blue triangles). This reported difference is scientifically validated because a difference is expected for CD8 and Dext high cells. We observe a probable cluster of transfected cells (blue triangles) in the rightmost plot where the data are projected along the CD8 and Dext markers.

4 Conclusion

In this work we have introduced a new multi-resolution Bayesian framework for testing and identifying two-sample differences based on a nonparametric process called the DMMT. This process uses Markov dependence to incorporate spatial clustering of differences, and randomized partitioning to achieve a data-adaptive multi-resolution partition sequence. We

have provided a recipe for inference based on forward-summation-backward-sampling type of recursive computation, and have showed how two-sample testing and identification of the differential structure can be carried out also based on recursive calculation. We have also established the large support property of the DMMT and proved the asymptotic consistency of the two-sample test based on this process.

The design of the DMMT process does not require either dimensionwise or dyadic partition sequences. Neither does it require the partition point to be in the middle of support in each dimension. More general partition schemes have been earlier considered by Ma and Wong (2011), and the DMMT can be directly extended to incorporate those more general partition systems. In this work we have deliberately chosen to introduce the DMMT with dimensionwise dyadic partitions to simplify the presentation and thereby highlighting the more unique features of the DMMT in comparison to other existing multi-resolution tests.

For the same reason we have introduced the DMMT in the context of comparing two data samples. The design of DMMT allows comparison across k samples ($k > 2$)—simply let the generative process of DMMT generate k distributions $(Q_1, \ldots, Q_k)$ simultaneously by drawing k assignment variables $Y_1(A), \ldots, Y_k(A)$ in the probability assignment step. The inferential recipe, computational algorithm, and theoretical results all remain valid.

Finally, we compare the computational efficiency of some of the methods considered in this work. The computation was executed on a single Intel(R) Core(TM) i7-3820 core with a 3.60GHz CPU clock. In the one-dimensional local shift example the median CPU times are $0.001s$ (KNN), $0.004s$ (DMMT) and $0.482s$ (Cramér). In the two-dimensional local shift example the median CPU times are $0.004s$ (KNN), $0.073s$ (DMMT) and $1.983s$ (Cramér). In the flow cytometry example the CPU times are $3085s$ (KNN), $7307s$ (DMMT), while we were unable to fit Cramér. (Note that although one can fit KNN to the data, it is not useful here because it cannot identify where the difference is located.). The computational

complexity of DMMT is linear in n, while those for both KNN and Cramér are quadratic. However, given the exponential nature of DMMT in p and k, efficient approximations are needed to scale it to high-dimensional problems.

Software

An R package implementing our method is available at https://github.com/jacsor/DMMT.

Acknowledgment

LM's research is supported by NSF grant DMS-1309057. Part of this work was completed while LM was a fellow, and JS a graduate fellow at Statistical and Applied Mathematical Sciences Institute (SAMSI). The authors want to thank Cliburn Chan for providing the flow cytometry data, which was made possible by grants from the Wallace Coulter Foundation and the NIH (P50-5P30 AI064518).

Appendix

A Numerical example 2

1. Local shift difference: $(p_1, \ldots, p_5) = (0.11, 0.16, 0.25, 0.39, 0.09), \delta = (1.0, 1.0)$,
   $\mu_1 = (9.0, 9.9), \mu_2 = (0.0, 4.4), \mu_3 = (-2.3, -9.7), \mu_4 = (3.4, 5.9), \mu_5 = (5.8, -9.5)$,
   $(\Sigma_1(1,1), \Sigma_1(1,2), \Sigma_1(2,2)) = (2.9, 0.5, 1.1), (\Sigma_2(1,1), \Sigma_2(1,2), \Sigma_2(2,2)) = (1.2, -0.6, 2.8)$,
   $(\Sigma_3(1,1), \Sigma_3(1,2), \Sigma_3(2,2)) = (2.3, -1.0, 1.7), (\Sigma_4(1,1), \Sigma_4(1,2), \Sigma_4(2,2)) = (1.1, -0.4, 2.9)$,
   $(\Sigma_5(1,1), \Sigma_5(1,2), \Sigma_5(2,2)) = (3.0, 0.2, 1.0)$.

2. Local dispersion difference: $(p_1, \ldots, p_5) = (0.19, 0.08, 0.33, 0.27, 0.13), \mu_1 = (0.9, -7.2), \mu_2 =$

$(-5.7, 3.3), \mu_3 = (-6.3, -2.1), \mu_4 = (7.5, -3.1), \mu_5 = (-3.1, 9.5)$,

$(\Sigma_1(1,1), \Sigma_1(1,2), \Sigma_1(2,2)) = (0.5, -0.1, 0.3), (\Sigma_2(1,1), \Sigma_2(1,2), \Sigma_2(2,2)) = (1.3, 0.7, 2.7)$,

$(\Sigma_3(1,1), \Sigma_3(1,2), \Sigma_3(2,2)) = (1.0, -0.3, 3.0), (\Sigma_4(1,1), \Sigma_4(1,2), \Sigma_4(2,2)) = (2.9, 0.5, 1.1)$,

$(\Sigma_5(1,1), \Sigma_5(1,2), \Sigma_5(2,2)) = (2.4, -0.9, 1.6)$.

3. Global shift difference: $(\Sigma(1,1), \Sigma(1,2), \Sigma(2,2)) = (2.9, 0.4, 1.1)$.

References

Baringhaus, L. and C. Franz (2004). On a new multivariate two-sample test. *Journal of Multivariate Analysis 88*(1), 190–206.

Bickel, P. J. (1969). A distribution free version of the smirnov two sample test in the p-variate case. *The Annals of Mathematical Statistics 40*(1), 1–23.

Chen, L., P. Dai, and W. Dou (2010). *MTSKNN: Multivariate two-sample tests based on K-nearest-neighbors*. R package version 0.0-5.

Chen, Y. and T. E. Hanson (2012). Bayesian nonparametric k-sample tests for censored and uncensored data. *Computational Statistics & Data Analysis*.

Crouse, M. S., R. D. Nowak, and R. G. Baraniuk (1998). Wavelet-based statistical signal processing using hidden markov models. *Signal Processing, IEEE Transactions on 46*(4), 886–902.

Ferguson, T. S. (1973). A bayesian analysis of some nonparametric problems. *The annals of statistics*, 209–230.

Franz, C. (2006). *cramer: Multivariate nonparametric Cramer-Test for the two-sample-problem*. R package version 0.8-1.

Henze, N. (1988). A multivariate two-sample test based on the number of nearest neighbor type coincidences. *The Annals of Statistics*, 772–783.

Holmes, C., F. Caron, J. Griffin, and D. A. Stephens (2012). Two-sample bayesian nonparametric hypothesis testing. *arXiv preprint arXiv:0910.5060*.

Lavine, M. (1992). Some aspects of pólya tree distributions for statistical modelling. *The Annals of Statistics*, 1222–1235.

Liu, J. S. (2008). *Monte Carlo strategies in scientific computing*. Springer.

Ma, L. and W. H. Wong (2011). Coupling optional pólya trees and the two sample problem. *Journal of the American Statistical Association 106*(496).

Schilling, M. F. (1986). Multivariate two-sample tests based on nearest neighbors. *Journal of the American Statistical Association 81*(395), 799–806.

Singh, S. K., B. Tummers, T. N. Schumacher, R. Gomez, K. L. Franken, E. M. Verdegaal, K. Laske, C. Gouttefangeas, C. Ottensmeier, M. J. Welters, et al. (2013). The development of standard samples with a defined number of antigen-specific t cells to harmonize t cell assays: a proof-of-principle study. *Cancer Immunology, Immunotherapy*, 1–13.

Wilks, S. S. (1938). The large-sample distribution of the likelihood ratio for testing composite hypotheses. *The Annals of Mathematical Statistics 9*(1), 60–62.

Wong, W. H. and L. Ma (2010). Optional pólya tree and bayesian inference. *The Annals of Statistics 38*(3), 1433–1459.

Supplementary Material

B.1 Proofs

Theorem 1.

Proof. First, assume without loss of generality that $\tilde{f}_t$ for $t = 1, 2$ are uniformly continuous because other densities can be approximated arbirtrarily well by uniformly continuous ones. Let

$$\delta_t(\epsilon) = \sup_{|x=y|<\epsilon} |\tilde{f}_t(x) - \tilde{f}_t(y)|.$$

Then, by uniformly continuity, $\delta_t(\epsilon) \downarrow 0$ as $\epsilon \downarrow 0$ for $t = 1, 2$. By Condition (1), for any $\epsilon > 0$ there is a partition of $\Omega = \cup_{i=1}^{I} A_i$ such that the diameter of each A_i is less than ϵ and $A_i \in \mathcal{A}^{(\infty)}$. By Conditions (2) and (3) there is a positive probability that this partition will arise during the partitioning process in a finite number of steps. Additionally, there is positive probability that the process will "merge" on each A_i. Then, the rest of the proof follows from the proof of Theorem 3 in Ma and Wong (2011). □

Lemma 1.

Proof. For a set A that arises during the partitioning process, consider an observation $x \in A$ of $\boldsymbol{x}_1$. Let $q_1(x|A) = q_1(x)/Q_1(A)$ and $q_0(x|A) = q_0(x)/Q_0(A)$, where $q_1 = dQ_1/d\mu$ and $q_0 = dQ_0/d\mu$. That is, $q_1(x|A)$ and $q_0(x|A)$ are the conditional density on A for Q_1 and Q_0, respectively. Then,

$$q_1(x|A) = \begin{cases} q_0(x|A) & \text{if } S(A) = s \\ \big(Y_1(A)\big)^{1(x \in A_l^{J(A)})} \big(1 - Y_1(A)\big)^{1(x \in A_r^{J(A)})} & \\ \quad \cdot \prod_{i \in \{l,r\}} q_1(x|A_i^{J(A)}) & \text{if } S(A) \in \{d, m\}. \end{cases}$$

Define $q_1(\boldsymbol{x}_1|A) = \prod_{x\in\boldsymbol{x}_1} q_1(x|A)$ and $q_0(\boldsymbol{x}_1|A) = \prod_{x\in\boldsymbol{x}_1} q_0(x|A)$, then

$$q_1(\boldsymbol{x}_1|A) = \begin{cases} q_0(\boldsymbol{x}_1|A) & \text{if } S(A) = s, \\ \big(Y_1(A)\big)^{n_1(A_l^{J(A)})}\big(1-Y_1(A)\big)^{n_1(A_r^{J(A)})} & \\ \quad \cdot \prod\limits_{i\in\{l,r\}} q_1(\boldsymbol{x}_1|A_i^{J(A)}) & \text{if } S(A) \in \{d,m\}, \end{cases}$$

where $n_1(A) = |\{x_{1,i} : x_{1,i} \in A,\ i = 1,2,\ldots,n_1\}|$. Similarly, define $q_2(\boldsymbol{x}_2)$, $q_2(\boldsymbol{x}_2|A)$ and $n_2(A)$. Finally, define $q(\boldsymbol{x}_1,\boldsymbol{x}_2|A) = q_2(\boldsymbol{x}_1|A)\cdot q_2(\boldsymbol{x}_2|A)$, then

$$q(\boldsymbol{x}_1,\boldsymbol{x}_2|A) = \begin{cases} q_0(\boldsymbol{x}_1|A)\cdot q_0(\boldsymbol{x}_2|A) & \text{if } S(A) = s, \\ \prod\limits_{t=1,2}\big(Y_t(A)\big)^{n_t(A_l^{J(A)})}\big(1-Y_t(A)\big)^{n_t(A_r^{J(A)})} & \\ \quad \cdot \prod\limits_{i\in\{l,r\}} q(\boldsymbol{x}_1,\boldsymbol{x}_2|A_i^{J(A)}) & \text{if } S(A) \in \{d,m\}. \end{cases}$$

Note that $q(\boldsymbol{x}_1,\boldsymbol{x}_2|A)$ is the conditional likelihood associated to the data points in A. In particular, when $S(A) = m$, then $Y_1(A) = Y_2(A) = Y(A)$, and so we can write it as

$$q(\boldsymbol{x}_1,\boldsymbol{x}_2|A) = \begin{cases} \prod_{x\in\boldsymbol{x}_1\cup\boldsymbol{x}_2} q_0(x|A) & \text{if } S(A) = s, \\ \big(Y(A)\big)^{n(A_l^{J(A)})}\big(1-Y(A)\big)^{n(A_r^{J(A)})} & \\ \quad \cdot \prod\limits_{i\in\{l,r\}} q(\boldsymbol{x}_1,\boldsymbol{x}_2|A_i^{J(A)}) & \text{if } S(A) = m, \\ \prod_{t=1,2}\big(Y_t(A)\big)^{n_t(A_l^{J(A)})}\big(1-Y_t(A)\big)^{n_t(A_r^{J(A)})} & \\ \quad \cdot q(\boldsymbol{x}_1,\boldsymbol{x}_2|A_i^{J(A)}) & \text{if } S(A) = d, \end{cases} \tag{B.8}$$

where $n(\cdot) = n_1(\cdot) + n_2(\cdot)$.

Define $Z(A,g,\boldsymbol{x}_1,\boldsymbol{x}_2)$ as the marginal likelihood conditional on A, given $E_1(A)$ and $S(A) = g$ for $g \in \mathcal{G}$. Then, we obtain

$$\Phi(A,g,\boldsymbol{x}_1,\boldsymbol{x}_2) = \sum_{h\in\mathcal{G}} \rho_{g,h}(A) Z(A,h,\boldsymbol{x}_1,\boldsymbol{x}_2). \tag{B.9}$$

If $S(A) = s$, then $q_t(\cdot|A) = q_0(\cdot|A)$, and so $Z(A, s, \boldsymbol{x}_1, \boldsymbol{x}_2) = \prod_{x \in \boldsymbol{x}_1 \cup \boldsymbol{x}_2} q_0(x|A)$. Otherwise, if $S(A) = g$, for $g \in \{d, m\}$, by integration of the right hand-side of (B.8), we obtain

$$\begin{aligned}
Z(A, m, \boldsymbol{x}_1, \boldsymbol{x}_2) &= \sum_{j=1}^{p} \lambda_j(A, m) E\Big[\big(Y(A)\big)^{n(A_l^j)}\big(1 - Y(A)\big)^{n(A_r^j)}\Big] \\
&\quad \cdot \prod_{i \in \{l,r\}} \int q(\boldsymbol{x}_1, \boldsymbol{x}_2|A_i^j)\pi\big(dq|E_1(A_i^j), E_{2,m}(A_i^j)\big) \\
&= \sum_{j=1}^{p} \lambda_j(A, m) \frac{D(\boldsymbol{\alpha}^j(A, m) + \boldsymbol{n}_1^j(A) + \boldsymbol{n}_2^j(A))}{D(\boldsymbol{\alpha}^j(A, m))} \cdot \prod_{i \in \{l,r\}} \Phi(A_i^j, m, \boldsymbol{x}_1, \boldsymbol{x}_2) \\
&= \sum_{j=1}^{p} Z_j(A, m, \boldsymbol{x}_1, \boldsymbol{x}_2),
\end{aligned}$$

and

$$\begin{aligned}
Z(A, d, \boldsymbol{x}_1, \boldsymbol{x}_2) &= \sum_{j=1}^{p} \lambda_j(A, d) E\Big[\prod_{t=1,2}\big(Y_t(A)\big)^{n_t(A_l^j)}\big(1 - Y_t(A)\big)^{n_t(A_r^j)}\Big] \\
&\quad \cdot \prod_{i \in \{l,r\}} \int q(\boldsymbol{x}_1, \boldsymbol{x}_2|A_i^j)\pi\big(dq|E_1(A_i^j), E_{2,d}(A_i^j)\big) \\
&= \sum_{j=1}^{p} \lambda_j(A, d) \prod_{t=1,2} \frac{D(\boldsymbol{\alpha}_t^j(A, d) + \boldsymbol{n}_t^j(A))}{D(\boldsymbol{\alpha}_t^j(A, d))} \cdot \prod_{i \in \{l,r\}} \Phi(A_i^j, d, \boldsymbol{x}_1, \boldsymbol{x}_2) \\
&= \sum_{j=1}^{p} Z_j(A, d, \boldsymbol{x}_1, \boldsymbol{x}_2).
\end{aligned}$$

□

Lemma 2.

Proof. The first claim holds because $\Phi(A, g, \boldsymbol{x}_1, \boldsymbol{x}_2)$ is the marginal likelihood, and so is equal to 1 if there are no data-points in A. The second claim follows from the DMMT self-similarity. For any region A that arises during the partitioning process, the DMMT restricted to A is a DMMT process with sample space $\Omega = A$, parameters restricted to A and its descendants, and baseline measure $Q_0(\cdot|A)$. The centering condition assumption

implies that $q_0(\cdot|A)$ is the predictive density. For a single data-point x in A, then $\Phi(A, g, \boldsymbol{x})$ is the predictive density at x. □

Theorem 2.

Proof. The proof is based on the results of Lemma 1. Note that the right-hand side of (B.9) is the sum of over $h \in \mathcal{G}$ of

$$\Pr\{\text{generate } \boldsymbol{x}_1, \boldsymbol{x}_2 | S(A) = h, S(\text{parent}(A)) = g\} \Pr\{S(A) = h | S(\text{parent}(A)) = g\},$$

for $g \in \mathcal{G}$ and $A \in \mathcal{A}^{(\infty)}$. Thus,

$$\Pr\left(S(A) = g | S(\text{parent}(A)) = h, \boldsymbol{x}_1, \boldsymbol{x}_2\right) = \rho_{g,h}(A|\boldsymbol{x}_1, \boldsymbol{x}_2) = \rho_{g,h}(A) \frac{Z(A, h, \boldsymbol{x}_1, \boldsymbol{x}_2)}{\Phi(A, g, \boldsymbol{x}_1, \boldsymbol{x}_2)},$$

for all $A \in \mathcal{A}^{(\infty)}$, $g, h \in \mathcal{G}$. Similarly, $Z_j(A, g, \boldsymbol{x}_1, \boldsymbol{x}_2)$ represents

$$\Pr\{\text{generate } \boldsymbol{x}_1, \boldsymbol{x}_2 | S(A) = g, \text{ split direction } j\} \Pr\{\text{ split direction } j | S(A) = g\},$$

for $g \in \mathcal{G}$, $j = 1, \ldots, p$ and $A \in \mathcal{A}^{(\infty)}$. Thus,

$$\Pr\left(J(A) = j | S(A) = g, \boldsymbol{x}_1, \boldsymbol{x}_2\right) = \frac{Z_j(A, g, \boldsymbol{x}_1, \boldsymbol{x}_2)}{Z(A, g, \boldsymbol{x}_1, \boldsymbol{x}_2)},$$

for all $A \in \mathcal{A}^{(\infty)}$, $g \in \{d, m\}$ and $j = 1, \ldots, p$. Finally, since the Beta distribution is conjugate to the Multinomial distribution, we have

$$\alpha_t(A, g|\boldsymbol{x}_1, \boldsymbol{x}_2) = \begin{cases} \alpha_t(A, d) + n_t(A) & \text{if } g = d \\ \alpha_t(A, m) + n_1(A) + n_2(A) & \text{if } g = m, \end{cases}$$

for all $A \in \mathcal{A}^{(\infty)}$, $g \in \{d, m\}$ and $t = 1, 2$. □

Lemma 3.

Proof. By self-similarity and conjugacy, we know that

$$(Q_1, Q_2)|(\boldsymbol{x}_1, \boldsymbol{x}_2, E_1(A), E_{2,g}(A))$$

is still a DMMT with initial state $\rho_{0,g} = 1$ and parameters defined by Theorem 2. Consider the event

$$\{q_1(\cdot|A) = q_2(\cdot|A)\} = \bigcup_{h \in \mathcal{G}} \big\{q_1(\cdot|A) = q_2(\cdot|A), S(A) = h\big\},$$

For $S(A) = s$ we have

$$\big\{q_1(\cdot|A) = q_2(\cdot|A), S(A) = s\big\} = \big\{q_1(\cdot|A) = q_2(\cdot|A) = q_0(\cdot|A), S(A) = s\big\},$$

and so

$$\int 1\{q_1(\cdot|A) = q_2(\cdot|A), S(A) = s\big\}\pi(dq|\boldsymbol{x}_1, \boldsymbol{x}_2, E_1(A), E_{2,g}(A)) = \rho_{g,s}(A|\boldsymbol{x}_1, \boldsymbol{x}_2).$$

For $S(A) = m$ we have

$$\big\{q_1(\cdot|A) = q_2(\cdot|A), S(A) = m\big\} = \bigcup_{j=1}^{p} \big\{q_1(\cdot|A) = q_2(\cdot|A), S(A) = m, J(A) = j\big\},$$

where

$$\begin{aligned}
&\big\{q_1(\cdot|A) = q_2(\cdot|A), S(A) = m, J(A) = j\big\} \\
&\qquad = \{Y(A)q_1(\cdot|A_l^j) + (1 - Y(A))q_1(\cdot|A_r^j) \\
&\qquad = Y(A)q_2(\cdot|A_l^j) + (1 - Y(A))q_2(\cdot|A_r^j), S(A) = m, J(A) = j\big\} \\
&\qquad = \big\{q_1(\cdot|A_l^j) = q_2(\cdot|A_l^j), q_1(\cdot|A_r^j) = q_2(\cdot|A_r^j), S(A) = m, J(A) = j\big\}
\end{aligned}$$

and so

$$\begin{aligned}
&\int 1\{q_1(\cdot|A) = q_2(\cdot|A), S(A) = m, J(A) = j\}\pi(dq|\boldsymbol{x}_1, \boldsymbol{x}_2, E_1(A), E_{2,g}(A)) \\
&\qquad = \rho_{g,m}(A|\boldsymbol{x}_1, \boldsymbol{x}_2)\lambda_j(A, m|\boldsymbol{x}_1, \boldsymbol{x}_2) \\
&\qquad\quad \cdot \prod_i \int 1\{q_1(\cdot|A_i^j) = q_2(\cdot|A_i^j)\}\pi(dq|\boldsymbol{x}_1, \boldsymbol{x}_2, E_1(A_i^j), E_{2,m}(A_i^j)) \\
&\qquad = \rho_{g,m}(A|\boldsymbol{x}_1, \boldsymbol{x}_2)\lambda_j(A, m|\boldsymbol{x}_1, \boldsymbol{x}_2) \prod_i \Psi(A_i^j, m, \boldsymbol{x}_1, \boldsymbol{x}_2).
\end{aligned}$$

Finally, for $S(A) = d$ we have

$$\{q_1(\cdot|A) = q_2(\cdot|A), S(A) = d\} = \bigcup_{j=1}^{p} \{q_1(\cdot|A) = q_2(\cdot|A), S(A) = d, J(A) = j\},$$

where

$$\begin{aligned}
&\{q_1(\cdot|A) = q_2(\cdot|A), S(A) = d, J(A) = j\} \\
&\qquad = \{Y_1(A)q_1(\cdot|A_l^j) + (1 - Y_1(A))q_1(\cdot|A_r^j) \\
&\qquad = Y_2(A)q_2(\cdot|A_l^j) + (1 - Y_2(A))q_2(\cdot|A_r^j), S(A) = m, J(A) = j\} \\
&\qquad = \{Y_1(A) = Y_2(A), q_1(\cdot|A_l^j) = q_2(\cdot|A_l^j), \\
&\qquad\quad q_1(\cdot|A_r^j) = q_2(\cdot|A_r^j), S(A) = m, J(A) = j\},
\end{aligned}$$

but the event has null probability since $Y_1(A), Y_2(A)$ are independent and absolutely continuous, then

$$\int 1\{q_1(\cdot|A) = q_2(\cdot|A), S(A) = d, J(A) = j\}\pi(dq|\boldsymbol{x}_1, \boldsymbol{x}_2, E_1(A), E_{2,g}(A)) = 0.$$

□

We observe two independent groups of i.i.d. samples $\boldsymbol{x_1} = (x_{1,1}, \ldots, x_{1,n_1})$ and $\boldsymbol{x_2} = (x_{2,1}, \ldots, x_{2,n_2})$ from two distributions Q_1 and Q_2, where $n = n_1 + n_2 \to \infty$, and $n_1/n \to \beta$ for some $\beta \in (0,1)$. Let (Q_1, Q_2) have a DMMT$(\boldsymbol{\rho}, \boldsymbol{\lambda}, \boldsymbol{\alpha}, Q_0)$. The two unknown distributions are P_1 and P_2. Define $P = \beta P_1 + (1-\beta)P_2$, $p_t^j = P_t^j(A_l^j|A)$, $p^j = P(A_l^j|A)$, $q^j = Q_0(A_i^j)/Q_0(A)$, $\hat{p}_t^j = n_t(A_l^j)/n_t(A)$ and $\hat{p}^j = n(A_l^j)/n(A)$ for $t = 1, 2$ and $j = 1, \ldots, p$.

Lemma 4. *For $A \in \mathcal{A}^{(\infty)}$ and $j = 1, \ldots, p$, define*

$$\Lambda_{m,d}(A, j, \boldsymbol{x}_1, \boldsymbol{x}_2) = \frac{D(\boldsymbol{\alpha}^j(A,m) + \boldsymbol{n}_1^j(A) + \boldsymbol{n}_2^j(A))/D(\boldsymbol{\alpha}^j(A,m))}{\prod_{t=1,2} D(\boldsymbol{\alpha}_t^j(A,d) + \boldsymbol{n}_t^j(A))/D(\boldsymbol{\alpha}_t^j(A,d))}.$$

Then,

1. $\log \Lambda_{m,d}(A, j, \boldsymbol{x}_1, \boldsymbol{x}_2)/\log n \xrightarrow{p} \eta'$ *for some* $\eta' > 0$ *if* $p_1^j = p_2^j$.

2. $\log \Lambda_{m,d}(A, j, \boldsymbol{x}_1, \boldsymbol{x}_2)/n \xrightarrow{p} \eta''$ *for some* $\eta'' < 0$ *if* $p_1^j \neq p_2^j$.

Proof. The case $p_1^j = p_2^j$ follows by Theorem 1 in Holmes et al. (2012), but we report the proof since it used to show the case $p_1^j \neq p_2^j$. Using Stirling's formula

$$D(x,y) = \frac{\Gamma(x)\Gamma(y)}{\Gamma(x+y)} \simeq \sqrt{2\pi}\frac{x^{x-1/2}y^{y-1/2}}{(x+y)^{x+y-1/2}}, \text{ for large } x, y, \tag{B.10}$$

we can approximate the ratio

$$\begin{aligned}
\Lambda_{m,d}(A, j, \boldsymbol{x}_1, \boldsymbol{x}_2) &\simeq \frac{\prod_{t=1,2} D(\boldsymbol{\alpha}_t^j(A,d))}{D(\boldsymbol{\alpha}^j(A,m))} \cdot \frac{1}{\sqrt{2\pi}} \cdot \frac{(\hat{p}^j)^{\alpha(A_l^j,m)-1/2)}(1-\hat{p}^j)^{\alpha(A_r^j,m)-1/2)}}{\prod_t (\hat{p}_t^j)^{\alpha_t(A_l^j,d)-1/2)}(1-\hat{p}_t^j)^{\alpha_t(A_r^j,d)-1/2)}} \\
&\quad \cdot \sqrt{\frac{n_1(A_l^j)n_2(A_l^j)}{n(A)}} \cdot \frac{(\hat{p}^j)^{n(A_l^j)}(1-\hat{p}^j)^{n(A_r^j)}}{\prod_t (\hat{p}_t^j)^{n_t(A_l^j)}(1-\hat{p}_t^j)^{n_t(A_r^j)}} \\
&\simeq C\sqrt{n(A)}\frac{(\hat{p}^j)^{n(A_l^j)}(1-\hat{p}^j)^{n(A_r^j)}}{\prod_t (\hat{p}_t^j)^{n_t(A_l^j)}(1-\hat{p}_t^j)^{n_t(A_r^j)}},
\end{aligned}$$

for some $C > 0$. Then, $\log \Lambda_{m,d}(A, j, \boldsymbol{x}_1, \boldsymbol{x}_2) \propto \frac{1}{2} \log n(A) + \log \Lambda$, where

$$\Lambda = (\hat{p}^j)^{n(A_l^j)}(1-\hat{p}^j)^{n(A_r^j)} / \prod_t (\hat{p}_t^j)^{n_t(A_l^j)}(1-\hat{p}_t^j)^{n_t(A_r^j)}.$$

Then Λ is the likelihood ratio for testing composite hypotheses $H_0 : p_1^j = p_2^j = p^j$ vs $H_1 : p_1^j, p_2^j \in (0,1)$. Under the null, $-2\log\Lambda \xrightarrow{d} \chi_1^2$ by Wilks (1938) and so $\log \Lambda_{m,d}(A, j, \boldsymbol{x}_1, \boldsymbol{x}_2)/\log n \xrightarrow{p} \eta'$ for some $\eta' > 0$.

Additionally, $\log\Lambda$ can be also written as $\log\Lambda = n(A) Y_{n(A)}$,

$$Y_{n(A)} \xrightarrow{p} \big(G(p^j) - \beta G(p_1^j) - (1-\beta) G(p_2^j)\big),$$

where

$$G(x) = x\log(x) + (1-x)\log(1-x) \quad \text{for } x \in (0,1).$$

If $p_1^j \neq p_2^j$, then $G(p^j) - \beta G(p_1^j) - (1-\beta)G(p_2^j) < 0$, since G is convex and $p^j = \beta p_1^j + (1-\beta)p_2^j$. Thus, $\log \Lambda_{m,d}(A, j, \boldsymbol{x}_1, \boldsymbol{x}_2)/n \xrightarrow{p} \eta''$ for some $\eta'' < 0$. □

Lemma 5. *Consider $A \in \mathcal{A}^{(\infty)}$ such that*

1. *$p_1^j = p_2^j$ for all $j = 1, \ldots, p$.*
2. *$\rho_{g,h}(A) \in (0,1)$ for all $g, h \in \{d, m\}$.*
3. *$\rho_{g,h}(A_i^j) \in (0,1)$ for all $g \in \{d, m\}$ and $h \in \mathcal{G}, i = l, r, j = 1, \ldots p$.*

Then, for all $g \in \mathcal{G}$,

$$\rho_{g,d}(A|\boldsymbol{x}_1, \boldsymbol{x}_2) \xrightarrow{p} 0.$$

Proof. For $g = s$, note that $\rho_{s,d}(A|\boldsymbol{x}_1, \boldsymbol{x}_2) = 0$, since $\rho_{s,d}(A) = 0$ by design. For $g \in \{m, d\}$,

$$\rho_{g,d}(A|\boldsymbol{x}_1, \boldsymbol{x}_2) = \frac{\rho_{g,d}(A) Z(A, d, \boldsymbol{x}_1, \boldsymbol{x}_2)}{\sum_{h \in \mathcal{G}} \rho_{g,h}(A) Z(A, h, \boldsymbol{x}_1, \boldsymbol{x}_2)} \leq \frac{\rho_{g,d}(A) Z(A, d, \boldsymbol{x}_1, \boldsymbol{x}_2)}{\rho_{g,m}(A) Z(A, m, \boldsymbol{x}_1, \boldsymbol{x}_2)}$$

Since $\rho_{g,d}(A)/\rho_{g,m}(A)$ is bounded for Condition (2), it is sufficient to that

$$\frac{Z(A,d,\boldsymbol{x}_1,\boldsymbol{x}_2)}{Z(A,m,\boldsymbol{x}_1,\boldsymbol{x}_2)} = \frac{\sum_j Z_j(A,d,\boldsymbol{x}_1,\boldsymbol{x}_2)}{\sum_j Z_j(A,m,\boldsymbol{x}_1,\boldsymbol{x}_2)} \xrightarrow{p} 0.$$

For any $j = 1,\ldots,p$

$$\frac{Z_j(A,d,\boldsymbol{x}_1,\boldsymbol{x}_2)}{Z_j(A,m,\boldsymbol{x}_1,\boldsymbol{x}_2)} = \Lambda_{m,d}(A,j,\boldsymbol{x}_1,\boldsymbol{x}_2)^{-1}\frac{\lambda_j(A,d)\prod_i \Phi(A_i^j,d,\boldsymbol{x}_1,\boldsymbol{x}_2)}{\lambda_j(A,m)\prod_i \Phi(A_i^j,m,\boldsymbol{x}_1,\boldsymbol{x}_2)},$$

where $\Lambda_{m,d}(A,j,\boldsymbol{x}_1,\boldsymbol{x}_2)^{-1} \xrightarrow{p} 0$ by Lemma 4, $\lambda_j(A,d)/\lambda_j(A,m)$ is bounded by conditions of Theorem 1, and , for $g^* = \text{argmax}_{g\in\mathcal{G}} Z(A_i^j,g,\boldsymbol{x}_1,\boldsymbol{x}_2)$,

$$\begin{aligned}\frac{\Phi(A_i^j,d,\boldsymbol{x}_1,\boldsymbol{x}_2)}{\Phi(A_i^j,m,\boldsymbol{x}_1,\boldsymbol{x}_2)} &= \frac{\sum_{g\in\mathcal{G}}\rho_{d,g}(A_i^j)Z(A_i^j,g,\boldsymbol{x}_1,\boldsymbol{x}_2)}{\sum_{h\in\mathcal{G}}\rho_{m,h}(A_i^j)Z(A_i^j,h,\boldsymbol{x}_1,\boldsymbol{x}_2)} \\ &\leq \frac{Z(A_i^j,g^*,\boldsymbol{x}_1,\boldsymbol{x}_2)}{\sum_{h\in\mathcal{G}}\rho_{m,h}(A_i^j)Z(A_i^j,h,\boldsymbol{x}_1,\boldsymbol{x}_2)} \leq \frac{1}{\rho_{m,g^*}(A_i^j)}\end{aligned}$$

is bounded since $\rho_{g,h}(A_i^j) \in (0,1)$ for all $g \in \{d,m\}, h \in \mathcal{G}$, $i = l,r$ and $j = 1,\ldots,p$. For any $\epsilon > 0$, define

$$E_j(\epsilon) = \left\{\omega : \frac{Z_j(A,d,\boldsymbol{x}_1,\boldsymbol{x}_2)}{Z_j(A,m,\boldsymbol{x}_1,\boldsymbol{x}_2)} < \frac{\epsilon}{p}\right\},$$

then on $\cap_j E_j(\epsilon)$,

$$\frac{\sum_j Z_j(A,d,\boldsymbol{x}_1,\boldsymbol{x}_2)}{\sum_j Z_j(A,m,\boldsymbol{x}_1,\boldsymbol{x}_2)} < \epsilon.$$

Since $Z_j(A,d,\boldsymbol{x}_1,\boldsymbol{x}_2)/Z_j(A,m,\boldsymbol{x}_1,\boldsymbol{x}_2) \xrightarrow{p} 0$, then $\forall\delta > 0, \exists N_j(\epsilon,\delta)$ such that $\Pr(E_j^c(\epsilon)) < \delta/p$, for any $n_1, n_2 > N_j(\epsilon,\delta)$. Then, for $N(\epsilon,\delta) = \max_j N_j(\epsilon,\delta)$

$$\Pr(\cap_j E_j(\epsilon)) = 1 - \Pr(\cup_j E_j^c(\epsilon)) \geq 1 - \sum_j \Pr(E_j^c(\epsilon)) \geq 1 - p\hat{\epsilon} = 1 - \delta.$$

and this implies that $\forall \epsilon > 0$ and $\forall \delta > 0$, $\exists\ N(\epsilon, \delta)$ such that, for any $n_1, n_2 > N(\epsilon, \delta)$,

$$\Pr\left(\frac{Z(A, d, \boldsymbol{x}_1, \boldsymbol{x}_2)}{Z(A, m, \boldsymbol{x}_1, \boldsymbol{x}_2)} < \epsilon\right) \geq 1 - \delta.$$

□

Theorem 3. (Consistency under the alternative)

Proof. First we find the tree topologies with highest marginal posterior probability under the null component of $\boldsymbol{Q}$. To this end, assume $(\boldsymbol{x}_1 \cup \boldsymbol{x}_2) \sim \tilde{Q}$ and $\tilde{Q} \sim \text{OPT}(\tilde{\boldsymbol{\rho}}, \tilde{\boldsymbol{\lambda}}, \tilde{\boldsymbol{\alpha}}, Q_0)$, where $\tilde{\rho}_0(A) = \rho_{m,s}(A)/(\rho_{m,m}(A) + \rho_{m,s}(A))$, $\tilde{\lambda}_j(A) = \lambda_j(A, m)$, and $\tilde{\boldsymbol{\alpha}}^j(A) = \boldsymbol{\alpha}^j(A, m)$ for all $A \in \mathcal{A}^{(\infty)}$ and $j = 1, \ldots, p$. Define $\pi^{(k)}$ a tree topology where all regions are stopped at most at level k, and call $\Pi^{(k)}$ the set of the $\pi^{(k)}$'s with highest marginal posterior probability as $n \to \infty$. Since there exists $A \in \mathcal{A}^{(\infty)}$ where $P_1(A_i^j|A) \neq P_2(A_i^j|A)$ and $\beta P_1(A_i^j|A) + (1 - \beta)P_2(A_i^j|A) \neq Q_0(A_i^j|A)$, by Theorem 4 in Wong and Ma (2010) for some large enough k, there is at least one non-stopped region B arising in $\pi^{(k)}$ such that $P_1(B_i^j|B) \neq P_2(B_i^j|B)$, for each $\pi^{(k)} \in \Pi^{(k)}$. Then, we show that the likelihood of "dividing" on B dominates the likelihood of "merging". In fact,

$$\frac{Z_j(B, m, \boldsymbol{x}_1, \boldsymbol{x}_2)}{Z_j(B, d, \boldsymbol{x}_1, \boldsymbol{x}_2)} = \frac{\lambda_j(B, m)}{\lambda_j(B, d)} \Lambda_{m,d}(B, j, \boldsymbol{x}_1, \boldsymbol{x}_2) \prod_i \frac{\Phi(B_i^j, m, \boldsymbol{x}_1, \boldsymbol{x}_2)}{\Phi(B_i^j, d, \boldsymbol{x}_1, \boldsymbol{x}_2)},$$

where $\log \Lambda_{m,d}(B, j, \boldsymbol{x}_1, \boldsymbol{x}_2) \xrightarrow{p} -\infty$ by Lemma 4, $\lambda_j(B, d)/\lambda_j(B, m)$ is bounded by Theorem 1, and

$$\frac{\Phi(B_i^j, m, \boldsymbol{x}_1, \boldsymbol{x}_2)}{\Phi(B_i^j, d, \boldsymbol{x}_1, \boldsymbol{x}_2)} \leq \max_{g \in \mathcal{G}} \frac{\rho_{m,g}(B_i^j)}{\rho_{d,g}(B_i^j)}$$

is bounded since $\rho_{d,g}(B_i^j) \in (0, 1)$ for all $g \in \mathcal{G}$. This implies that

$$\Pr(H_0|\boldsymbol{x}_1, \boldsymbol{x}_2) \xrightarrow{p} 0 \text{ under } P_1^{(\infty)} \times P_2^{(\infty)}.$$

□

Theorem 4. (Consistency under the null)

Proof. For any set $A \in \mathcal{A}^l$ for $l > k$, we have that $\Psi(A, g, \boldsymbol{x}_1, \boldsymbol{x}_2) = 1$, since $\rho_{g,d}(A) = 0$ by design. For any set $A \in \mathcal{A}^{(k)}$, if $\Psi(A_i^j, g, \boldsymbol{x}_1, \boldsymbol{x}_2) \xrightarrow{p} 1$ for any $j = 1, \ldots, p$, and $i \in \{l, r\}$, then, by Slutsky's theorem,

$$\Psi(A, g, \boldsymbol{x}_1, \boldsymbol{x}_2) \xrightarrow{p} \rho_{g,s}(A|\boldsymbol{x}_1, \boldsymbol{x}_2) + \rho_{g,m}(A|\boldsymbol{x}_1, \boldsymbol{x}_2) \sum_j \lambda_j(A, m|\boldsymbol{x}_1, \boldsymbol{x}_2),$$

for any $g \in \{d, m\}$. Additionally, $\sum_j \lambda_j(A, m|\boldsymbol{x}_1, \boldsymbol{x}_2) = 1$, and $\big(\rho_{g,s}(A|\boldsymbol{x}_1, \boldsymbol{x}_2) + \rho_{g,m}(A|\boldsymbol{x}_1, \boldsymbol{x}_2)\big) \xrightarrow{p} 1$ by Condition (1), Condition (2) and Lemma 5. Then,

$$\Psi(A, g, \boldsymbol{x}_1, \boldsymbol{x}_2) \xrightarrow{p} 1 \quad \text{and} \quad \Pr(H_0|\boldsymbol{x}_1, \boldsymbol{x}_2) \xrightarrow{p} 1.$$

□

B.2 Example 1 in numerical examples

In Figure 7 we provide an analysis of sensitivity to the prior choice for the local shift difference example. We plot $\Pr(H_0|\boldsymbol{x}_1, \boldsymbol{x}_2)$ for different choices of the hyperparameters of the transition probability matrix under the null (red) and under the alternative (blue), showing that the results are robust to the prior specification. Similar results are obtained for the other scenarios and examples and so are not reported.

References

Baringhaus, L. and C. Franz (2004). On a new multivariate two-sample test. *Journal of Multivariate Analysis 88*(1), 190–206.

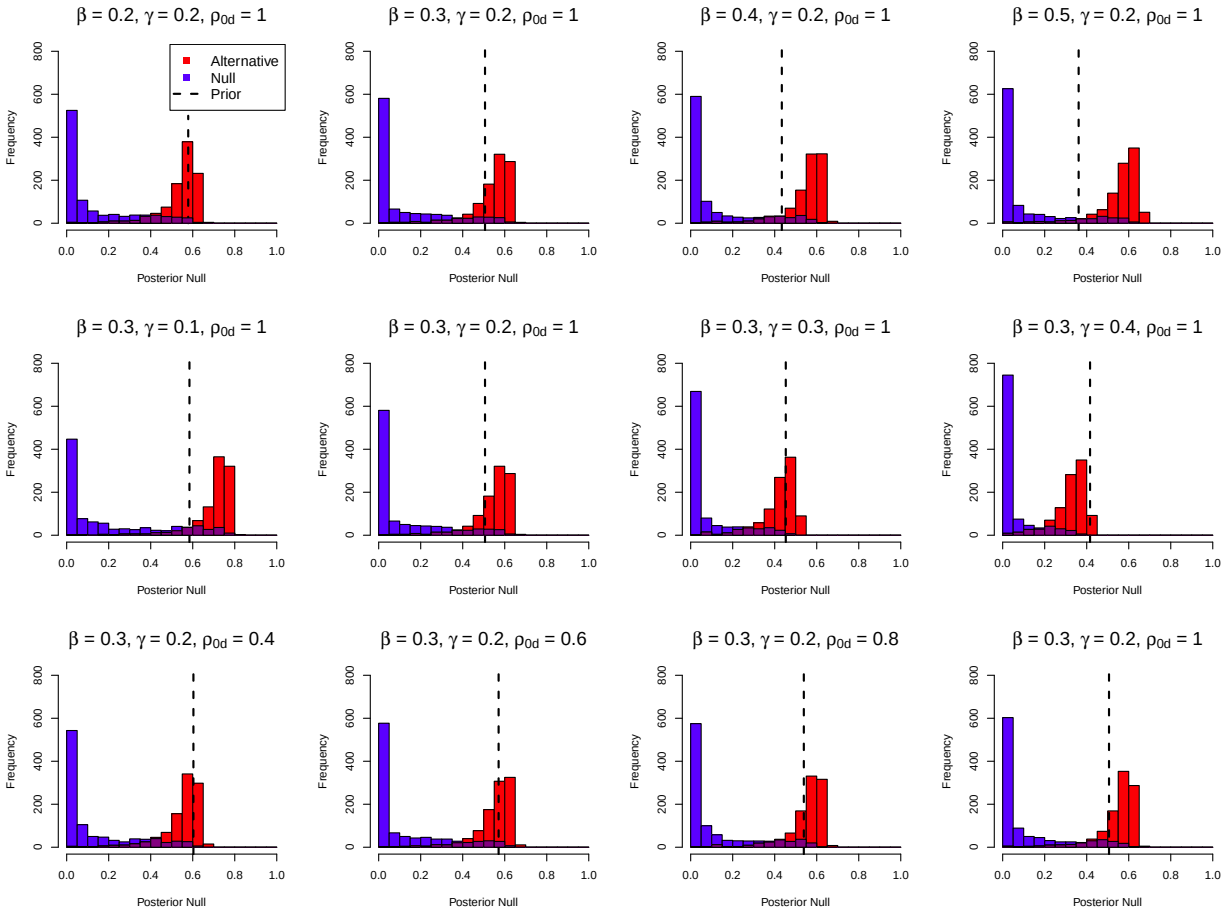
β = 0.2, γ = 0.2, ρ0d = 1
β = 0.3, γ = 0.2, ρ0d = 1
β = 0.4, γ = 0.2, ρ0d = 1
β = 0.5, γ = 0.2, ρ0d = 1
β = 0.3, γ = 0.1, ρ0d = 1
β = 0.3, γ = 0.2, ρ0d = 1
β = 0.3, γ = 0.3, ρ0d = 1
β = 0.3, γ = 0.4, ρ0d = 1
β = 0.3, γ = 0.2, ρ0d = 0.4
β = 0.3, γ = 0.2, ρ0d = 0.6
β = 0.3, γ = 0.2, ρ0d = 0.8
β = 0.3, γ = 0.2, ρ0d = 1
Alternative
Null
Prior
Frequency
Posterior Null

Figure 7: Bayes Factors for the local shift difference scenario in $\mathbb{R}^1$ for different choices of the hyperparameters of the transition probability matrix. In red the results under the null and in blue the results under the alternative.

Bickel, P. J. (1969). A distribution free version of the smirnov two sample test in the p-variate case. *The Annals of Mathematical Statistics 40*(1), 1–23.

Chen, L., P. Dai, and W. Dou (2010). *MTSKNN: Multivariate two-sample tests based on K-nearest-neighbors*. R package version 0.0-5.

Chen, Y. and T. E. Hanson (2012). Bayesian nonparametric k-sample tests for censored and uncensored data. *Computational Statistics & Data Analysis*.

Crouse, M. S., R. D. Nowak, and R. G. Baraniuk (1998). Wavelet-based statistical signal processing using hidden markov models. *Signal Processing, IEEE Transactions on 46*(4), 886–902.

Ferguson, T. S. (1973). A bayesian analysis of some nonparametric problems. *The annals of statistics*, 209–230.

Franz, C. (2006). *cramer: Multivariate nonparametric Cramer-Test for the two-sample-problem*. R package version 0.8-1.

Henze, N. (1988). A multivariate two-sample test based on the number of nearest neighbor type coincidences. *The Annals of Statistics*, 772–783.

Holmes, C., F. Caron, J. Griffin, and D. A. Stephens (2012). Two-sample bayesian nonparametric hypothesis testing. *arXiv preprint arXiv:0910.5060*.

Lavine, M. (1992). Some aspects of pólya tree distributions for statistical modelling. *The Annals of Statistics*, 1222–1235.

Liu, J. S. (2008). *Monte Carlo strategies in scientific computing*. Springer.

Ma, L. and W. H. Wong (2011). Coupling optional pólya trees and the two sample problem. *Journal of the American Statistical Association 106*(496).

Schilling, M. F. (1986). Multivariate two-sample tests based on nearest neighbors. *Journal of the American Statistical Association 81*(395), 799–806.

Singh, S. K., B. Tummers, T. N. Schumacher, R. Gomez, K. L. Franken, E. M. Verdegaal, K. Laske, C. Gouttefangeas, C. Ottensmeier, M. J. Welters, et al. (2013). The development of standard samples with a defined number of antigen-specific t cells to harmonize t cell assays: a proof-of-principle study. *Cancer Immunology, Immunotherapy*, 1–13.

Wilks, S. S. (1938). The large-sample distribution of the likelihood ratio for testing composite hypotheses. *The Annals of Mathematical Statistics 9*(1), 60–62.

Wong, W. H. and L. Ma (2010). Optional pólya tree and bayesian inference. *The Annals of Statistics 38*(3), 1433–1459.